

Understanding Transient Combustion Phenomena in Low-NO_x Gas Turbines

Project DE-FE0025495, Oct. 2015 – Sept. 2018 (now Sept. 2019 with NCE)

Program Monitor: Mark Freeman

PI: Jacqueline O'Connor, Ph.D.

Co-PI: Dom Santavicca, Ph.D.

RE: Stephen Peluso, Ph.D.

Graduate students: Dan Doleiden, Wyatt Culler,
Adam Howie, John Strollo

Undergraduates: Olivia Sekulich

Industry Partner: GE Global Research
Keith McManus, Tony Dean, Fei Han

Mechanical and Nuclear Engineering
Pennsylvania State University
sites.psu.edu/rfdl/



Overview of presentation

- Project motivation and approach
- Review of previous results
- Year 3 major results:
 - Stability bifurcation during long-duration transients
 - Damping quantification
 - Local flame dynamics
- Conclusions and next steps

Overview of presentation

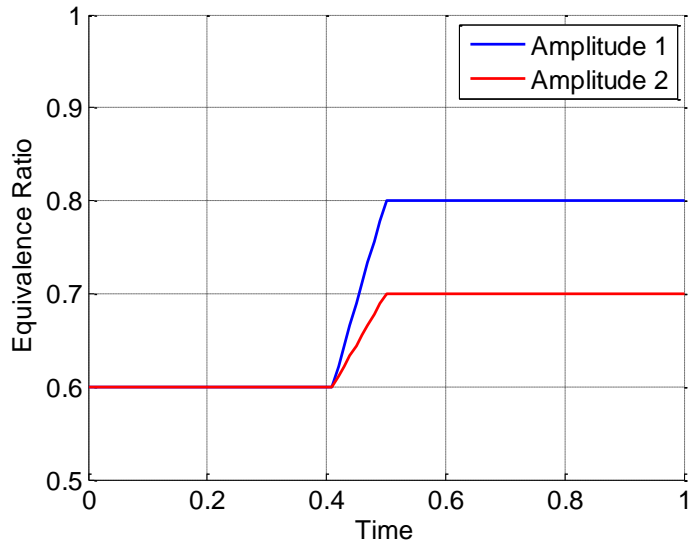
- Project motivation and approach
- Review of previous results
- Year 3 major results:
 - Stability bifurcation during long-duration transients
 - Damping quantification
 - Local flame dynamics
- Conclusions and next steps

Objective of the program is to *understand, quantify, and predict* combustion instability during transient operation

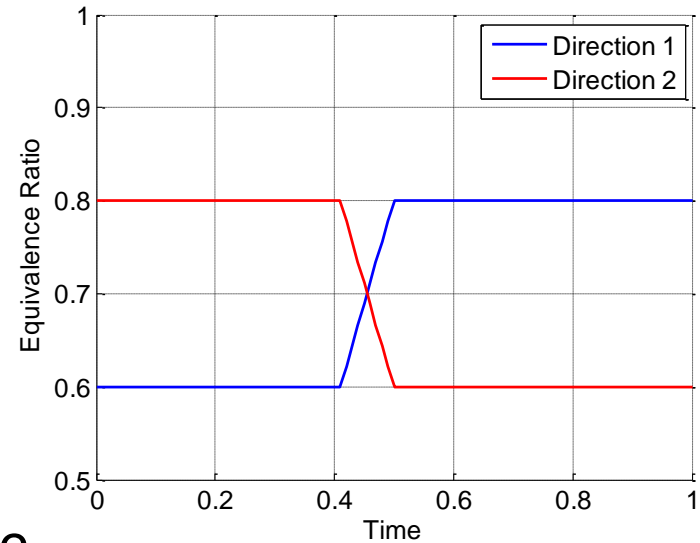
- Two major deliverables for the program:
 1. Fundamental understanding of flow and flame behavior during combustion transients and mechanisms for transition to instability
 2. Development of a stability prediction or quantification framework

The transients will be quantified using three different metrics:
amplitude, timescale, and direction

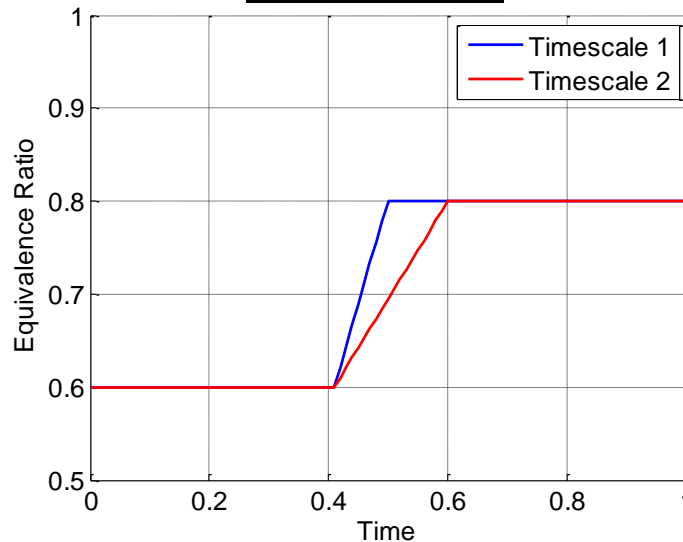
Amplitude



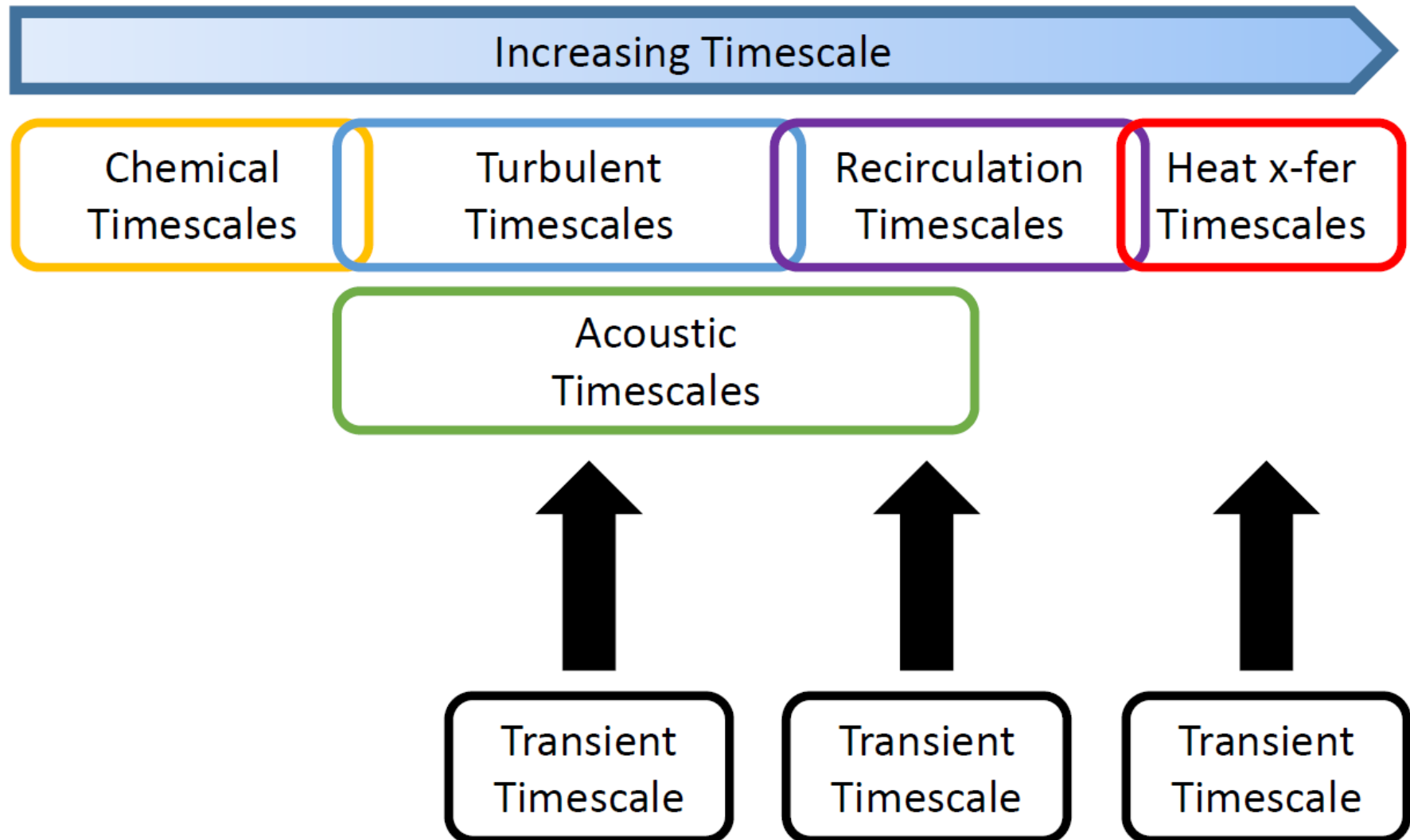
Direction



Timescale



Varying the transient timescales allows for different processes to equilibrate during the transient, changing the path

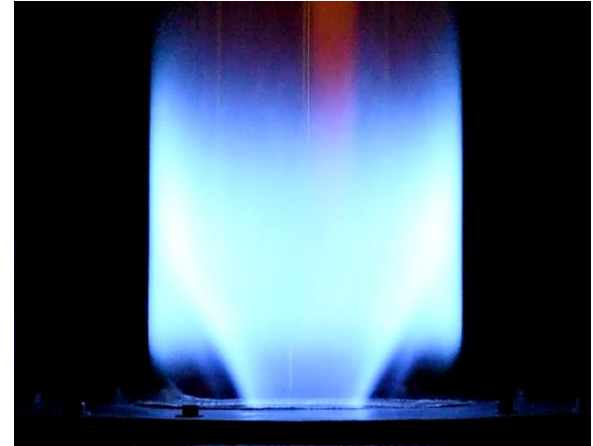


Project Management Plan – progress to date

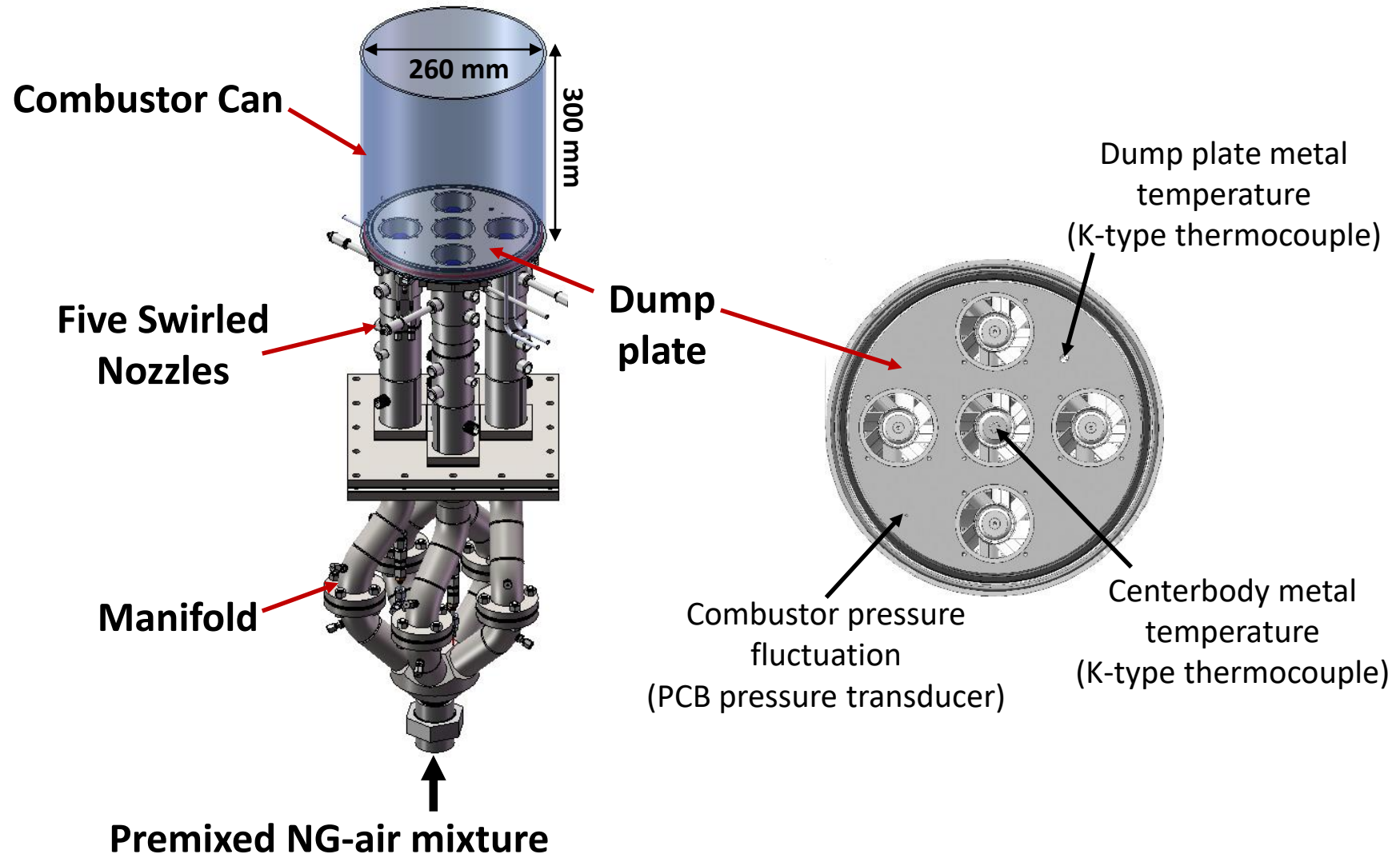
- Task 1 – Project management and planning
- Task 2 – Modification of current experimental facility with monitoring diagnostics and new hardware for transient control
- Task 3 – Map combustor timescales at target operating points
- Task 4 – Design of transient experiments
- Task 5 – Fuel split transients (multi-nozzle combustor)
- Task 6 – Equivalence ratio transients (single- and multi-nozzle)
- Task 7 – Fuel composition transients (single- and multi-nozzle)
- Task 8 – Data analysis and determination of prediction/quantification framework

Three types of transients are being considered in both multi-nozzle and single-nozzle combustors

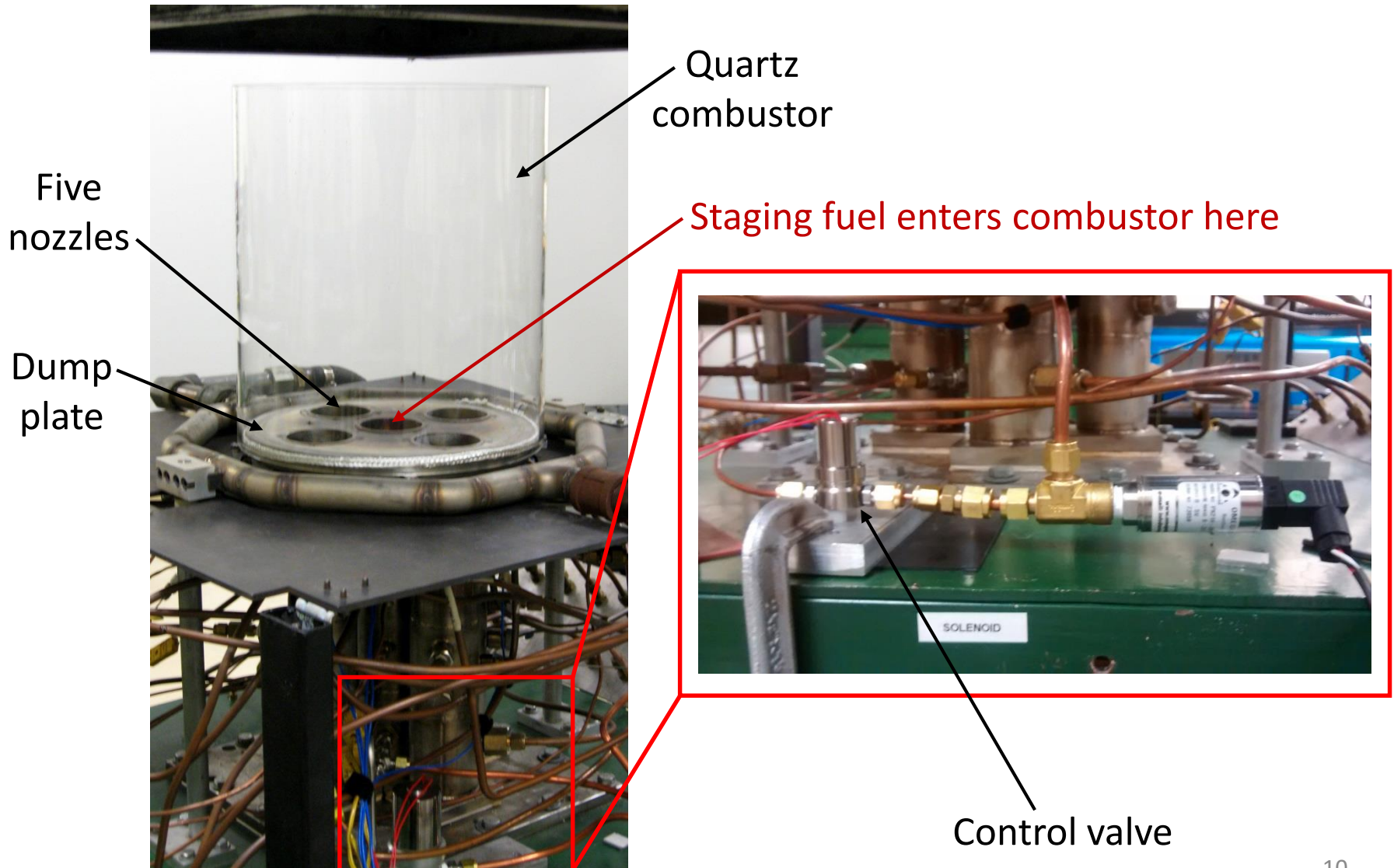
- Fuel-staging transients
 - Multi-nozzle only
- Equivalence ratio transients
 - Multi- and single-nozzle
- Fuel composition transients
 - Multi- and single-nozzle



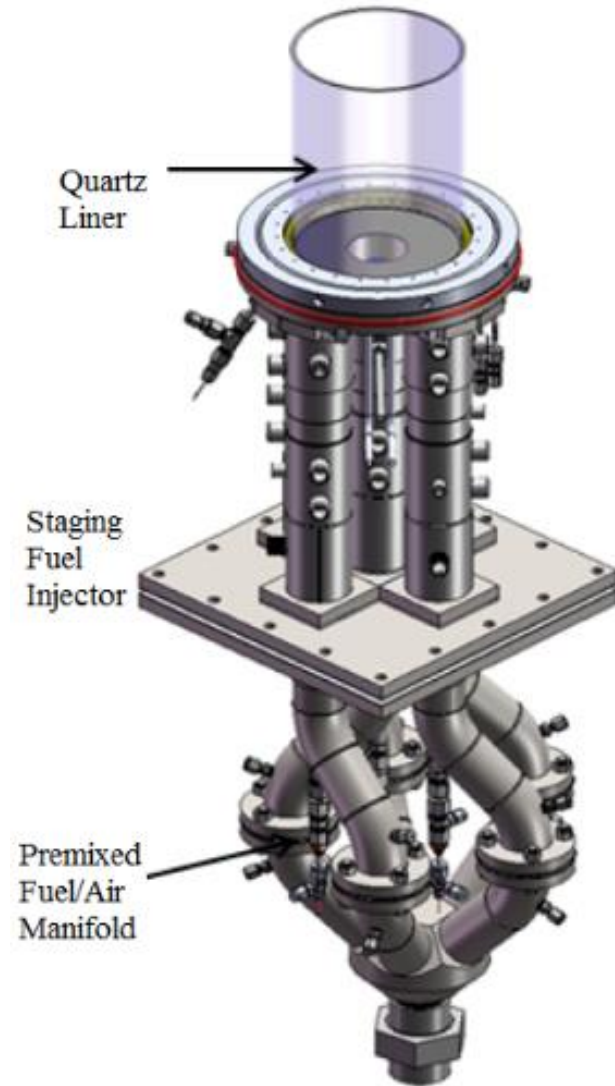
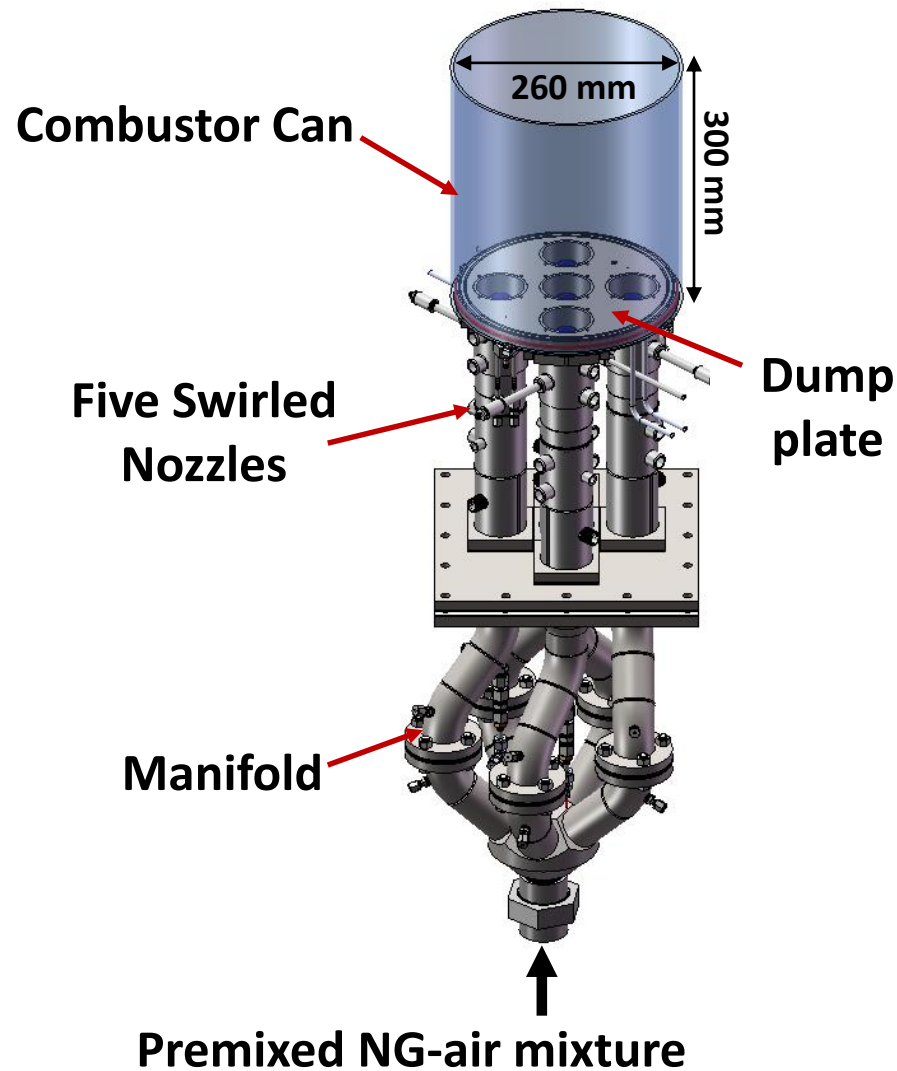
Experimental facilities include both a single-nozzle and multi-nozzle combustor, fuel splitting on multi-nozzle only



Hardware modification focused on a valve with linear actuation to control fuel flow transients for fuel-splitting studies



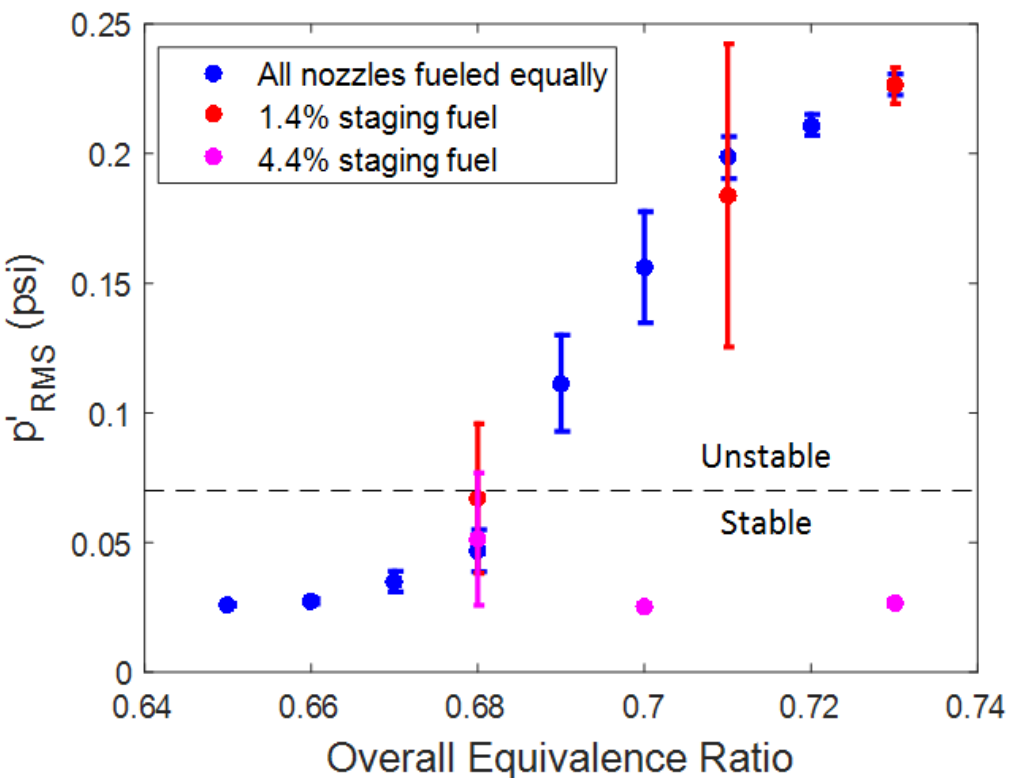
Single-nozzle combustor is created by plugging four nozzles and using a smaller quartz liner with the same dump ratio



Overview of presentation

- Project motivation and approach
- Review of previous results
- Year 3 major results:
 - Stability bifurcation during long-duration transients
 - Damping quantification
 - Local flame dynamics
- Conclusions and next steps

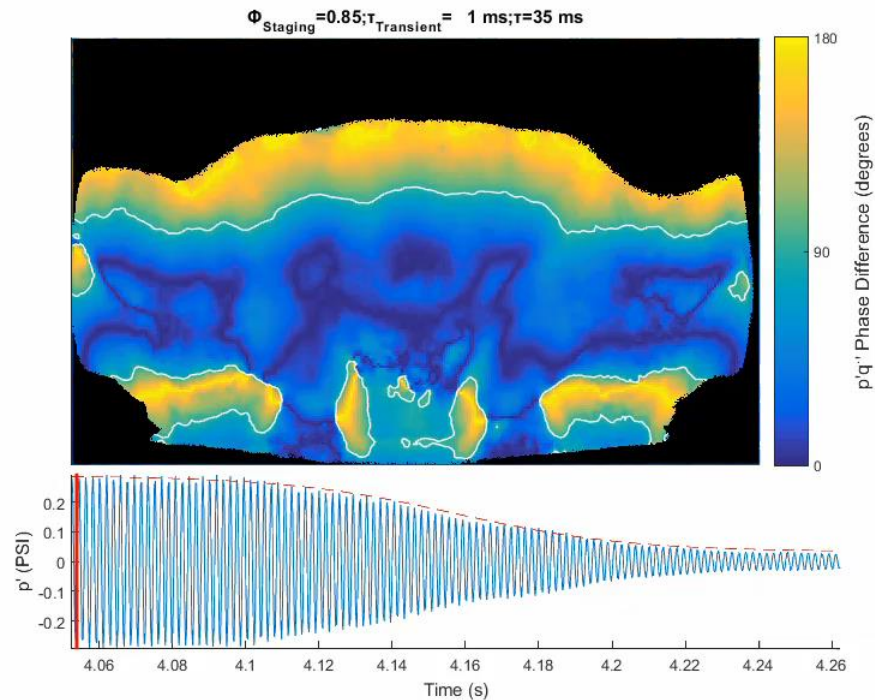
Major Result #1: Fuel staging works both in axisymmetric and non-axisymmetric configurations



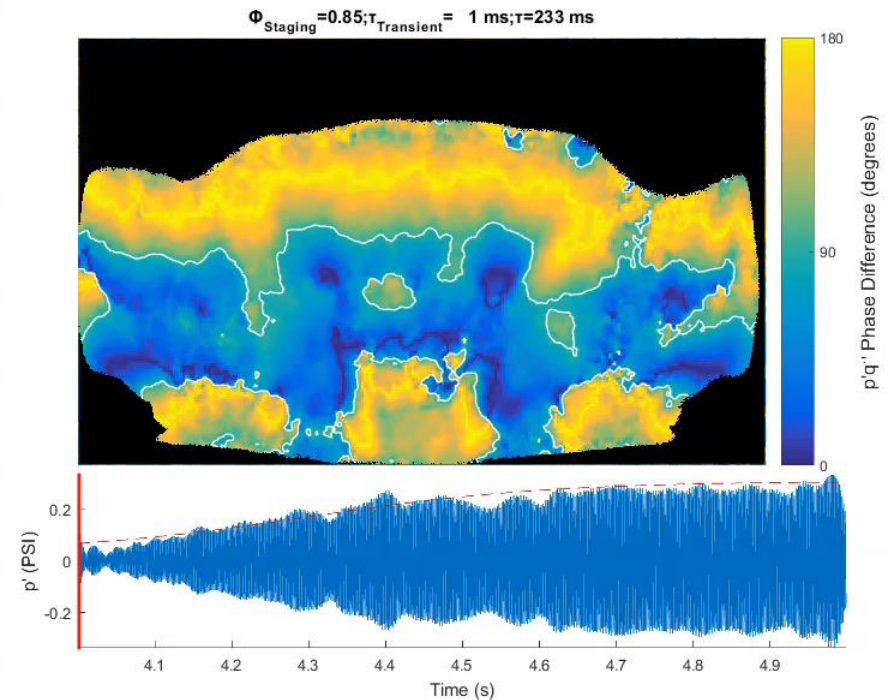
Nozzle	Bifurcation Equivalence Ratio
Center	0.79
Nozzle 1	0.85
Nozzle 2	0.83
Nozzle 3	0.80
Nozzle 4	0.78

Major Result #2: While instability decay is smooth, instability onset takes longer and is intermittent – direction matters!

Instability Decay



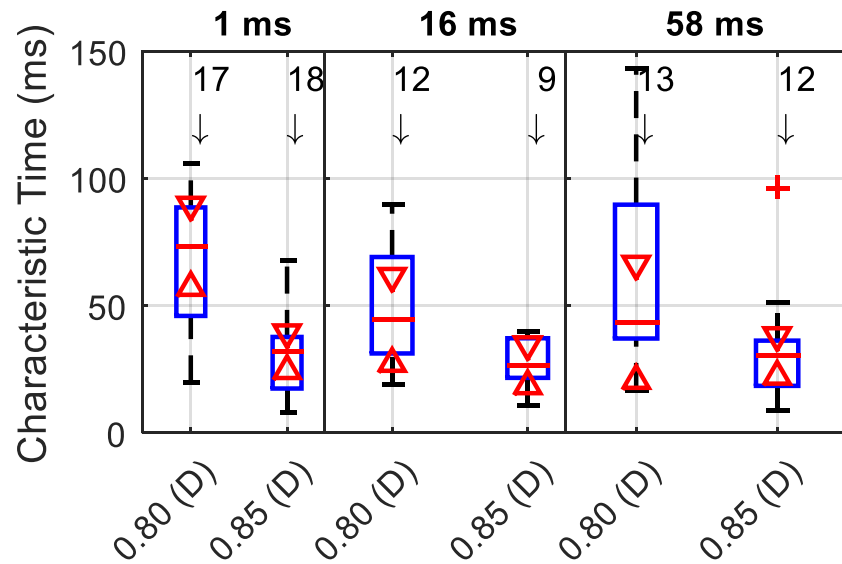
Instability Onset



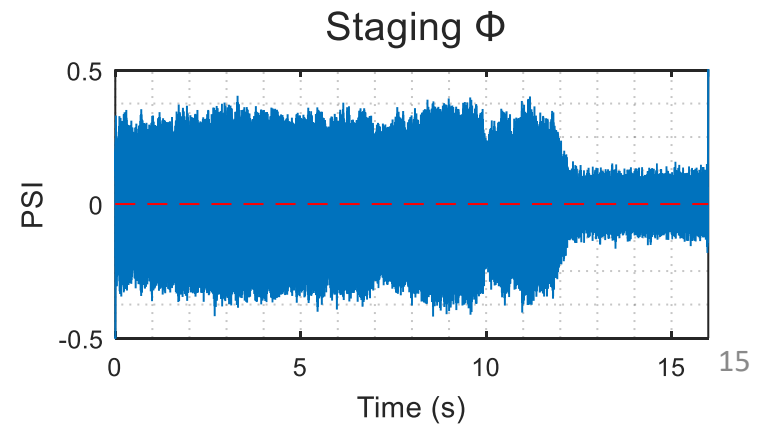
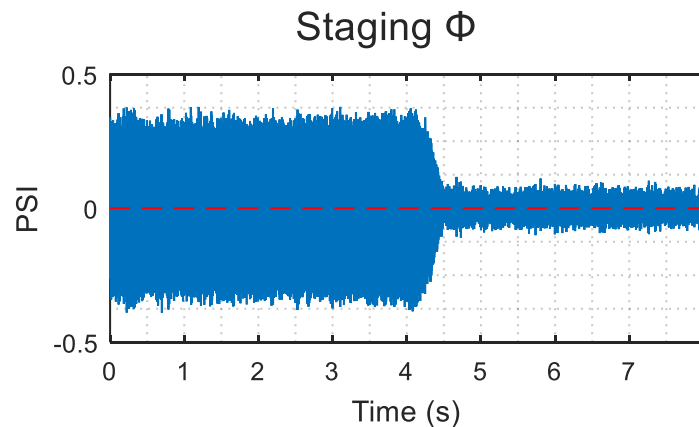
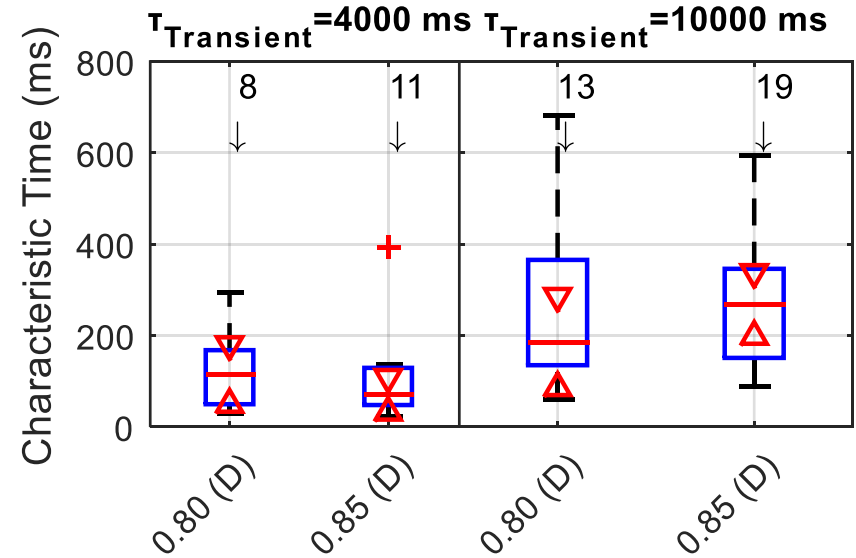
Culler, W., Chen, X., Samarasinghe, J., Peluso, S., Santavicca, D., O'Connor, J., (2018) "The effect of variable fuel staging transients on self-excited instabilities in a multiple-nozzle combustor," *Combustion and Flame*, vol. 194, pg. 472-484

Major Result #3: Time-scale of a transient matters in the multi-nozzle combustor, and heat transfer likely plays a role

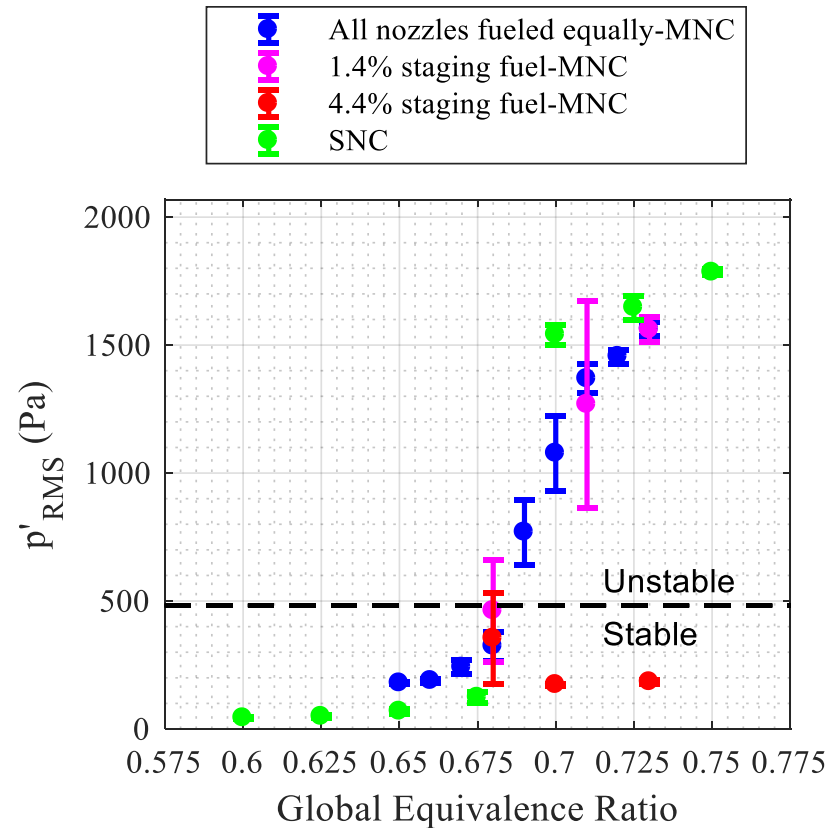
Short Timescales



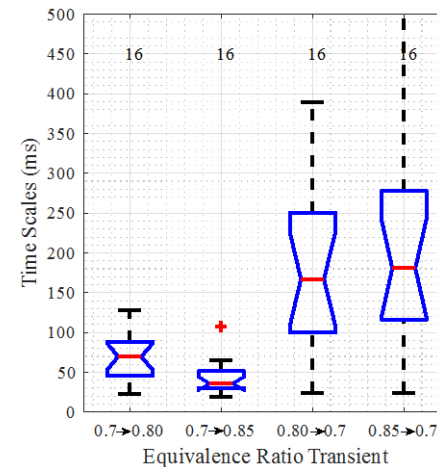
Long Timescales



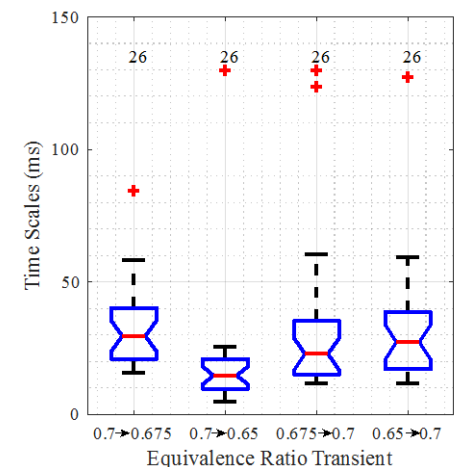
Major Result #4: Most significant difference between the single- and multi-nozzle instability is transient timescales



Multi-Nozzle Transients



Single-Nozzle Transients



Chen, X., Culler, W., Peluso, S., Santavicca, D., O'Connor, J., (2018) "Comparison of equivalence ratio transients on combustion instability in single-nozzle and multi-nozzle combustors," ASME Turbo Expo

Major findings and remaining questions

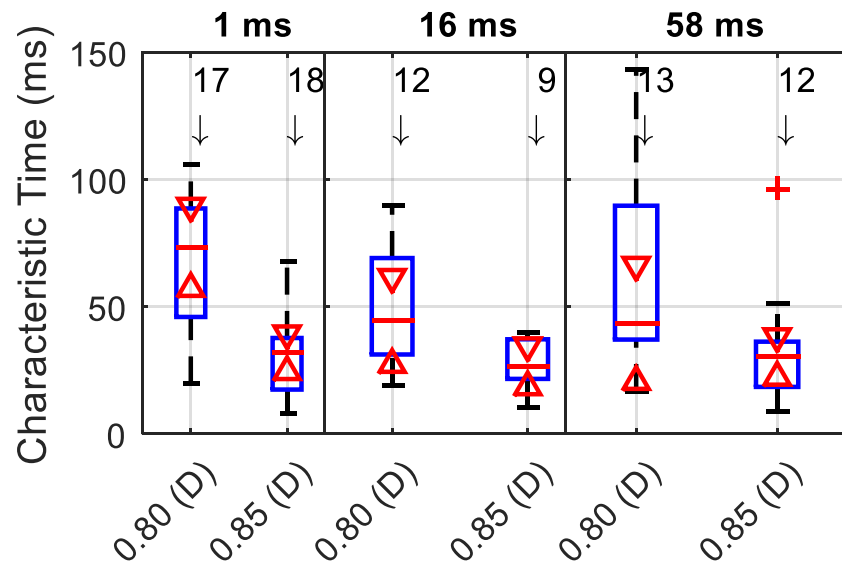
1. Fuel staging works both in axisymmetric and non-axisymmetric configurations
 - *What is driving the differences between staging efficacy?*
2. While instability decay is smooth, instability onset takes longer and is intermittent – direction matters!
 - *How do we quantify the intermittency we see during onset?*
3. Time-scale of a transient matters in the multi-nozzle combustor, and heat transfer likely plays a role
 - *What are the flame dynamics occurring during the transition?*
4. Most significant difference between the single- and multi-nozzle instability is transient timescales
 - *How much of a role does flame/flow interaction play on the transient physics?*

Overview of presentation

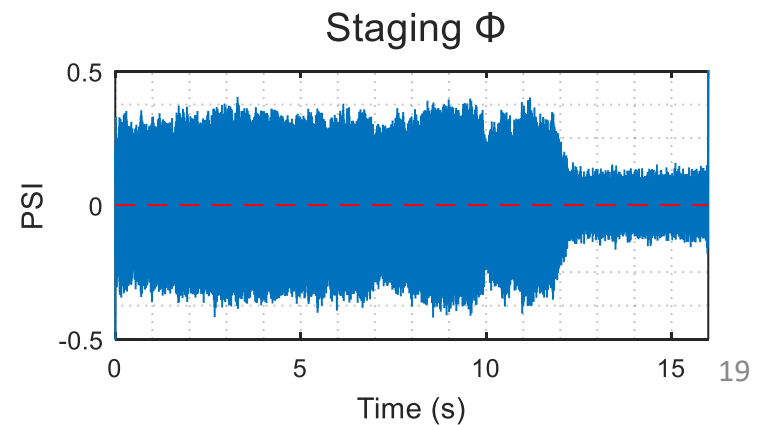
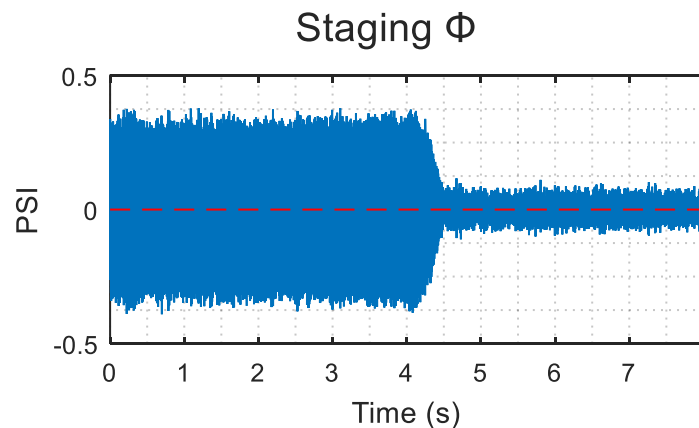
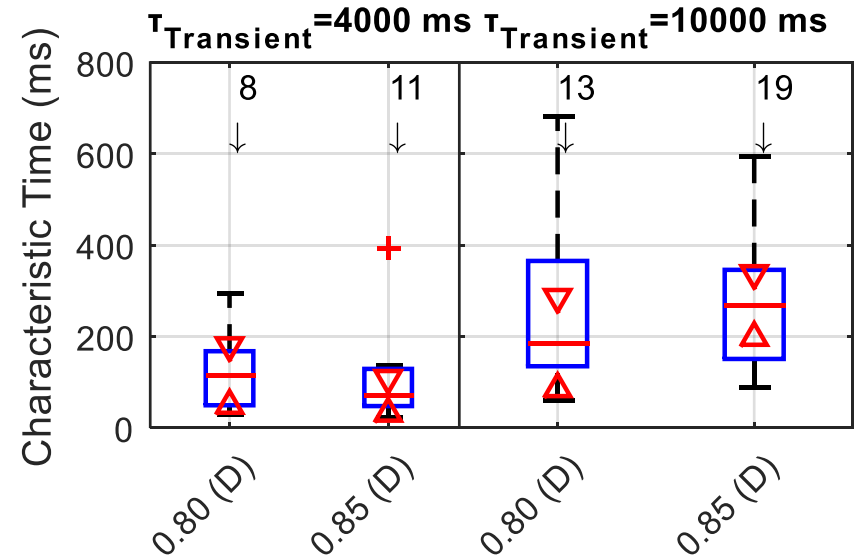
- Project motivation and approach
- Review of previous results
- Year 3 major results:
 - Stability bifurcation during long-duration transients
 - Damping quantification
 - Local flame dynamics
- Conclusions and next steps

Short- and long-duration transient behavior was different – long-duration timescales did not scale with the actuation time

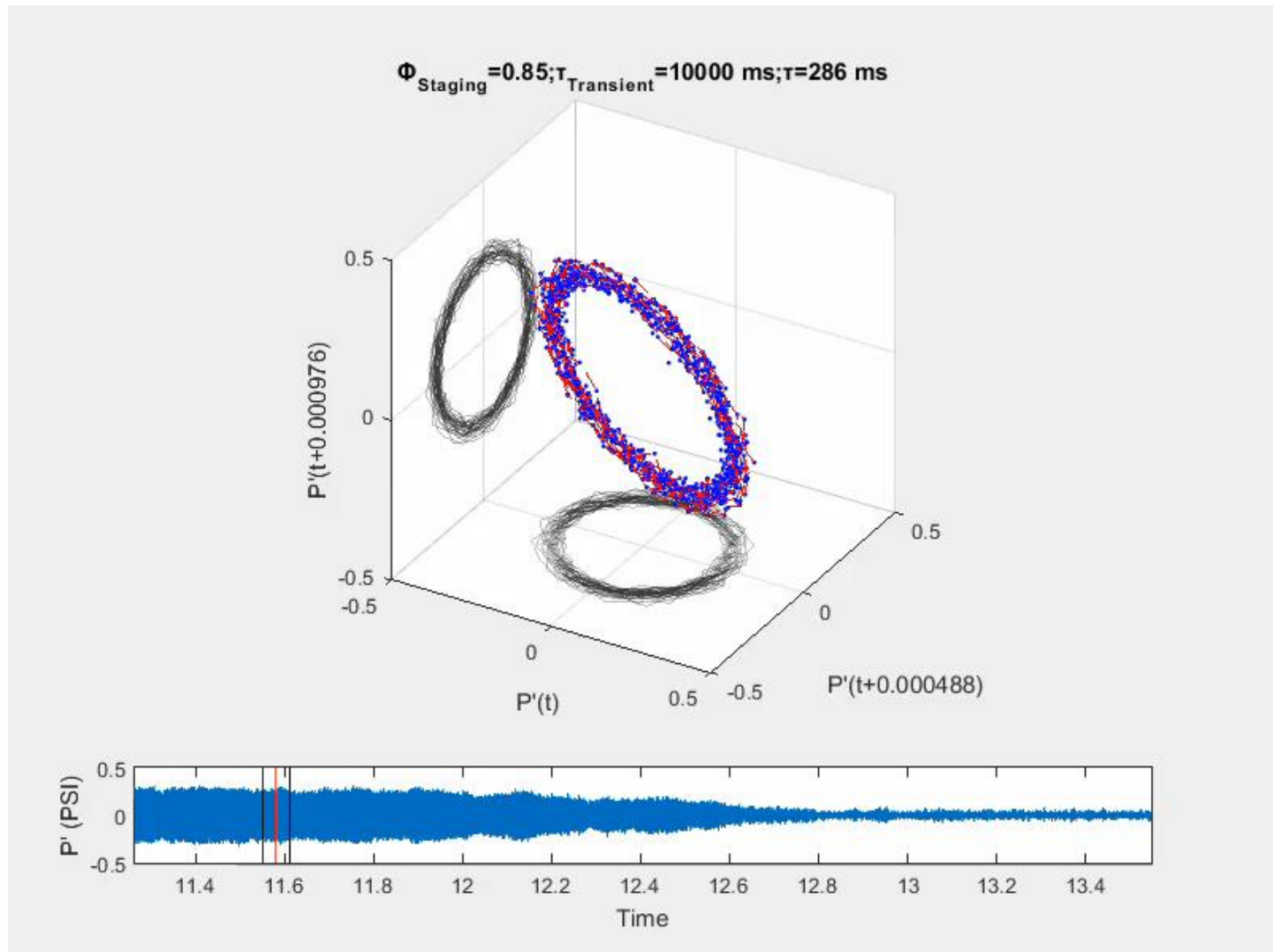
Short Timescales



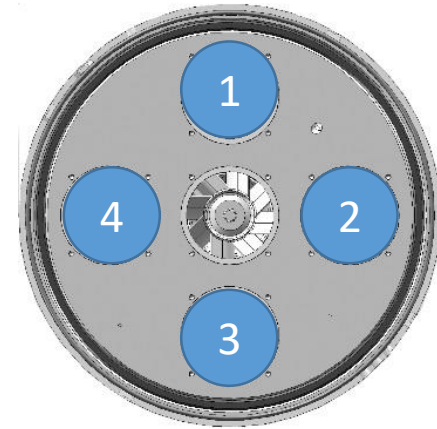
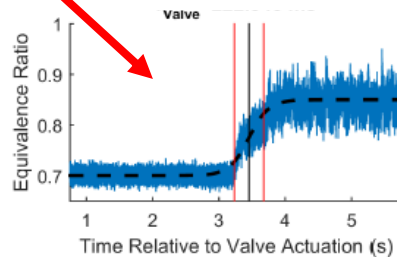
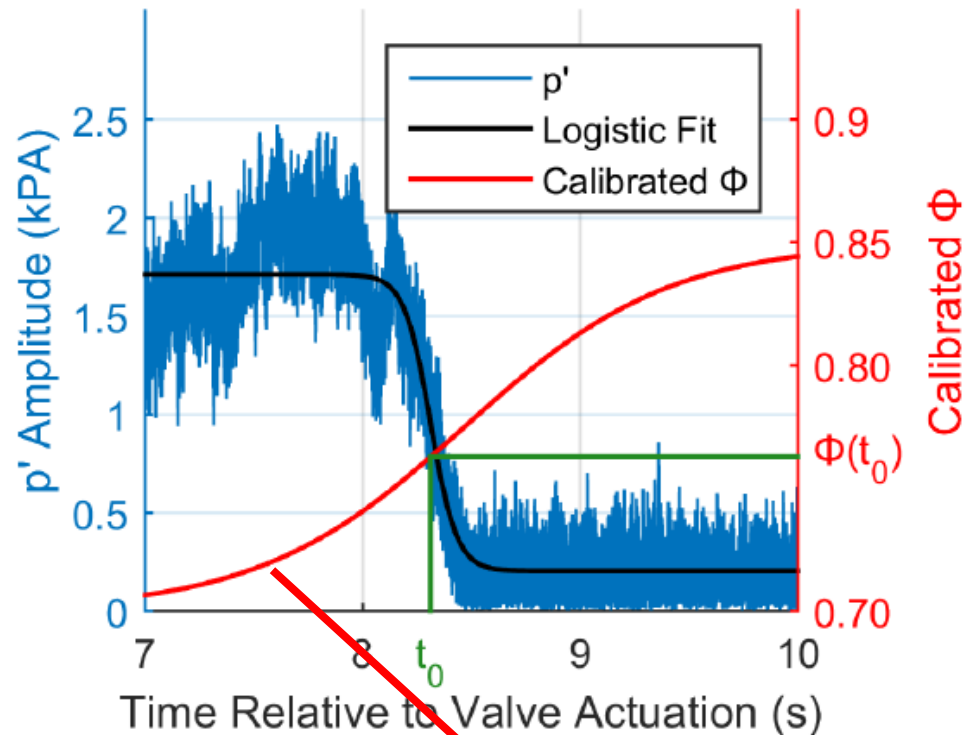
Long Timescales



The long-duration tests were done slowly enough; system responded quasi-steadily, allowing heat transfer to “keep up”



This steady-state behavior allowed us to see the instability evolve in real time and identify the stability bifurcation point



Nozzle	Bifurcation Equivalence Ratio
Center	0.79
Nozzle 1	0.85
Nozzle 2	0.83
Nozzle 3	0.80
Nozzle 4	0.78

Overview of presentation

- Project motivation and approach
- Review of previous results
- Year 3 major results:
 - Stability bifurcation during long-duration transients
 - Damping quantification
 - Local flame dynamics
- Conclusions and next steps

Quantifying the thermoacoustic damping of the combustor is a way to understand the efficacy of fuel staging

Thermoacoustic system model

$$\sum_{n=1}^N [\ddot{\eta}_n + 2\alpha_n \dot{\eta}_n + \omega_n^2 \eta_n = \dot{q}'_n]$$

Heat release rate model

$$\dot{q}'_n = 2\beta_n \dot{\eta}_n - \kappa \eta_n^2 \dot{\eta}_n$$

Van der Pol oscillator

$$\ddot{\eta}_n + 2(\alpha_n - \beta_n + \kappa \eta_n^2) \dot{\eta}_n + \omega_n^2 \eta_n = \zeta(t)$$

Acoustic
damping



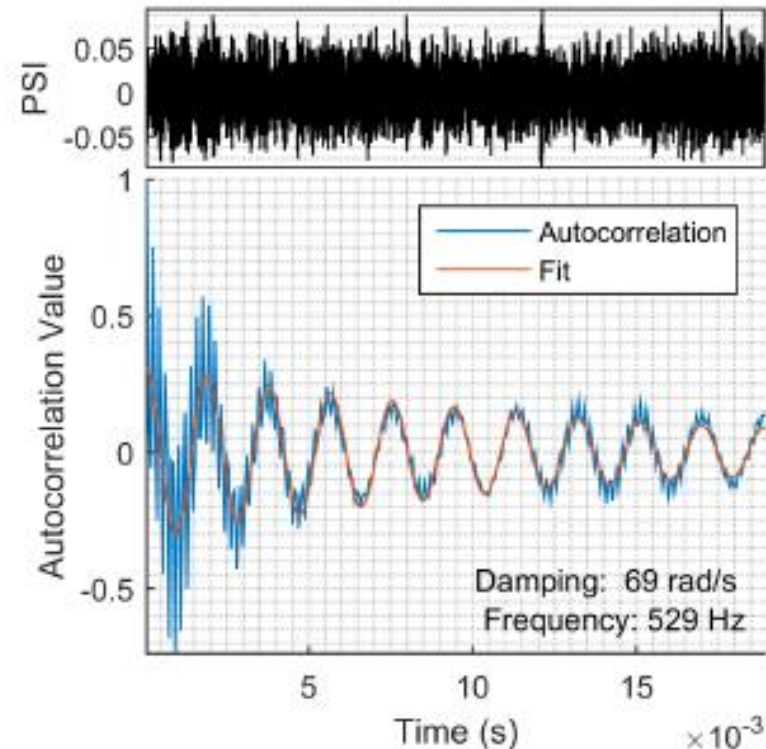
Flame
driving



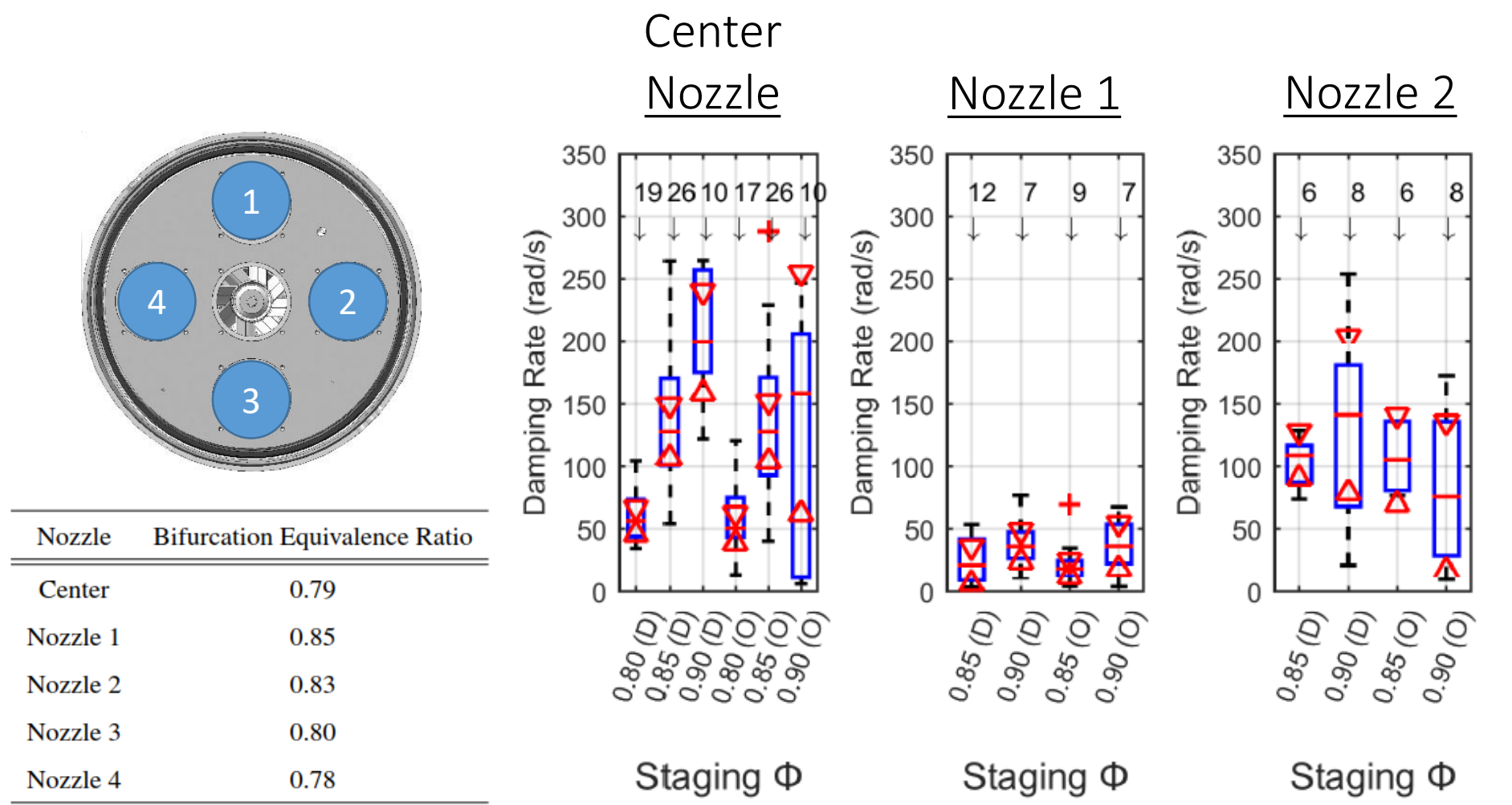
Thermoacoustic
damping

Autocorrelation function

$$k_{\eta_n \eta_n}(\tau) = \exp(-\nu_n \tau) \cos(\omega_n \tau)$$



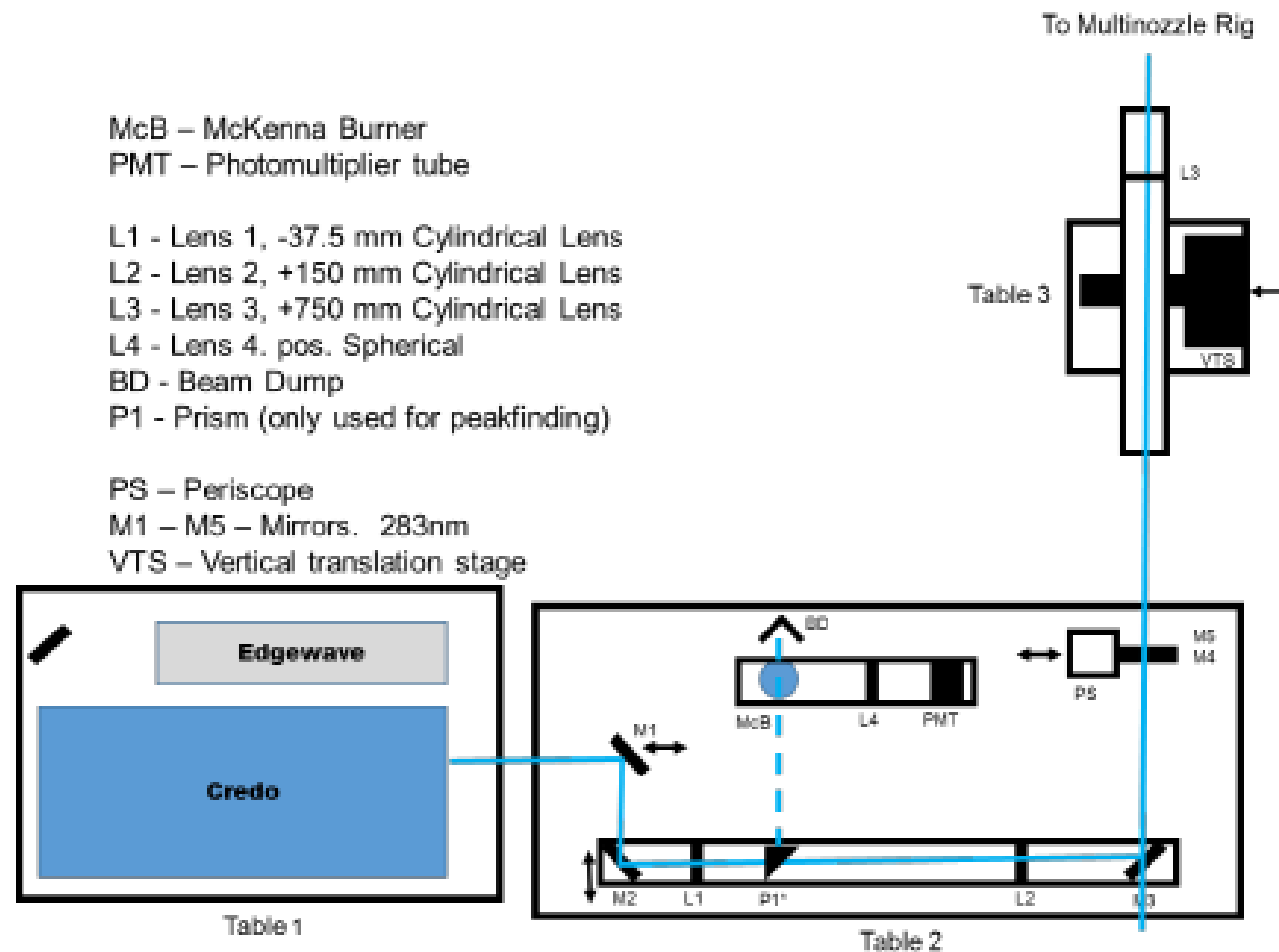
Damping is a more reliable metric for quantifying suppression because of variations in the bifurcation equivalence ratio



Overview of presentation

- Project motivation and approach
- Review of previous results
- Year 3 major results:
 - Stability bifurcation during long-duration transients
 - Damping quantification
 - Local flame dynamics
- Conclusions and next steps

Local flame dynamics were measured with a high-speed OH-PLIF system at a rate of 10 kHz, imaging two of five flames

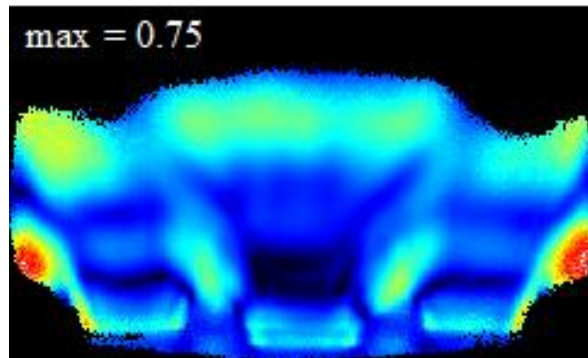


OH-PLIF provides localized flame oscillation information, which we link back to the heat release rate oscillations

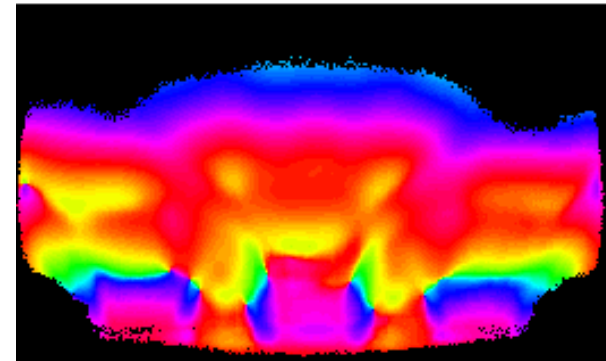


The first goal of this analysis was to test the hypothesis about phase cancellation as the suppression mechanism with staging

Unstable:

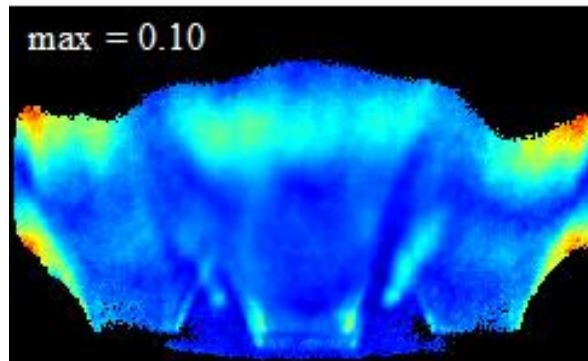


$$\varphi_{\text{outer}} = 0.70, \varphi_{\text{middle}} = 0.70$$
$$\varphi_{\text{overall}} = 0.70$$

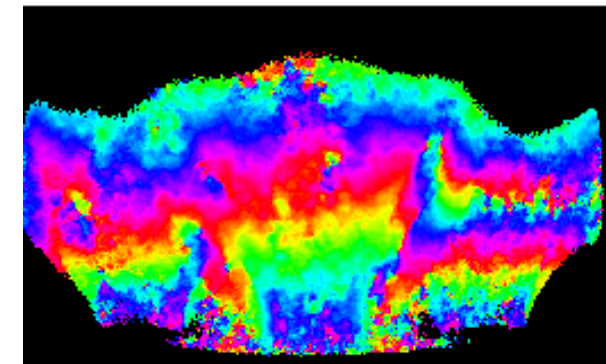


$$\varphi_{\text{outer}} = 0.70, \varphi_{\text{middle}} = 0.70$$
$$\varphi_{\text{overall}} = 0.70$$

Stable:



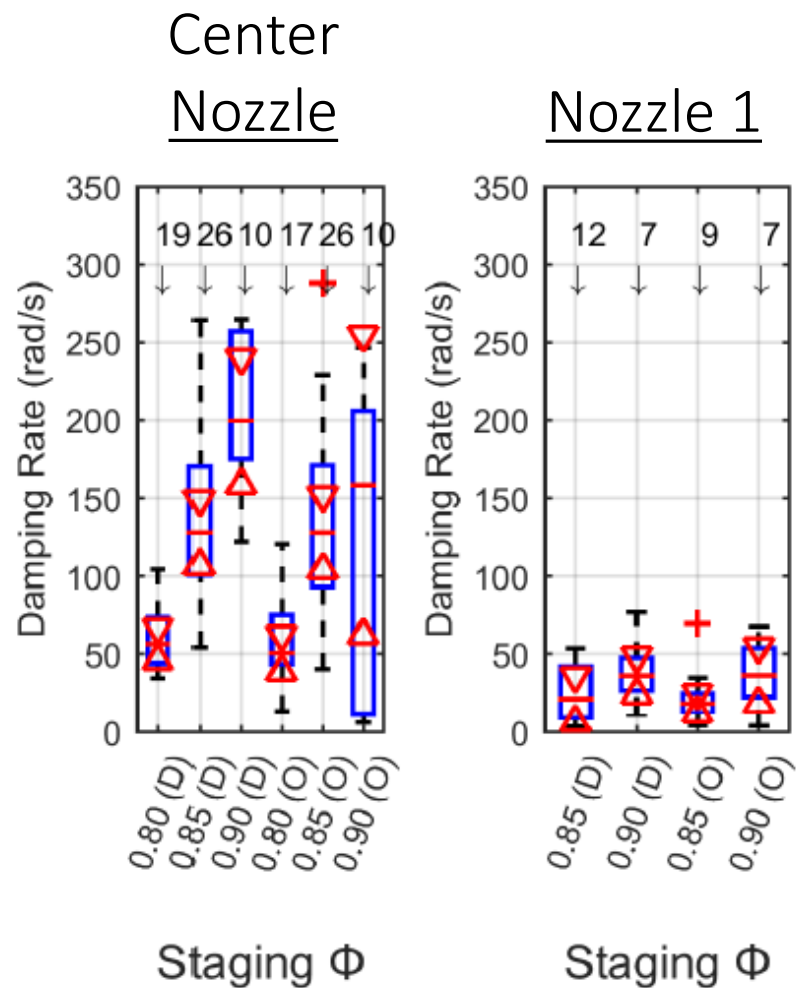
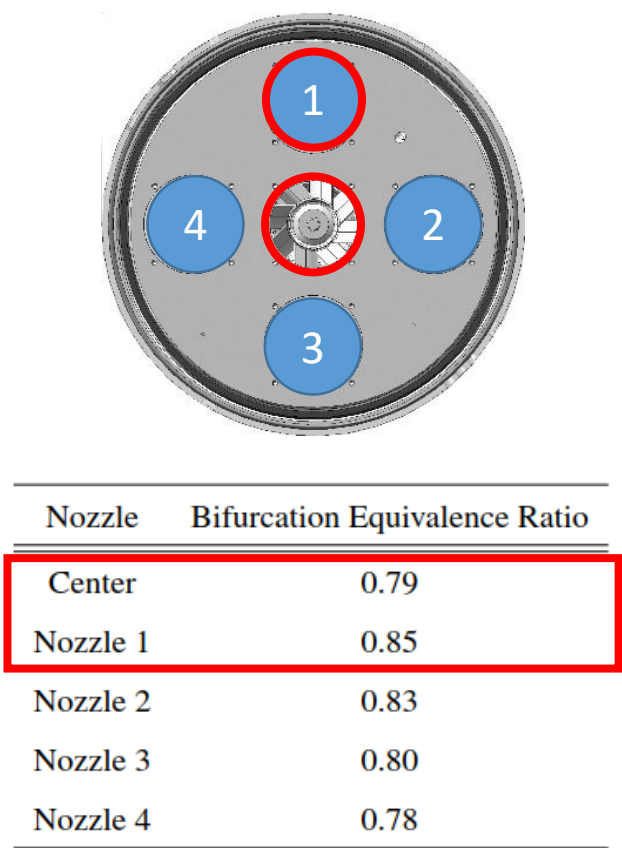
$$\varphi_{\text{outer}} = 0.70, \varphi_{\text{middle}} = 0.86$$
$$\varphi_{\text{overall}} = 0.73$$



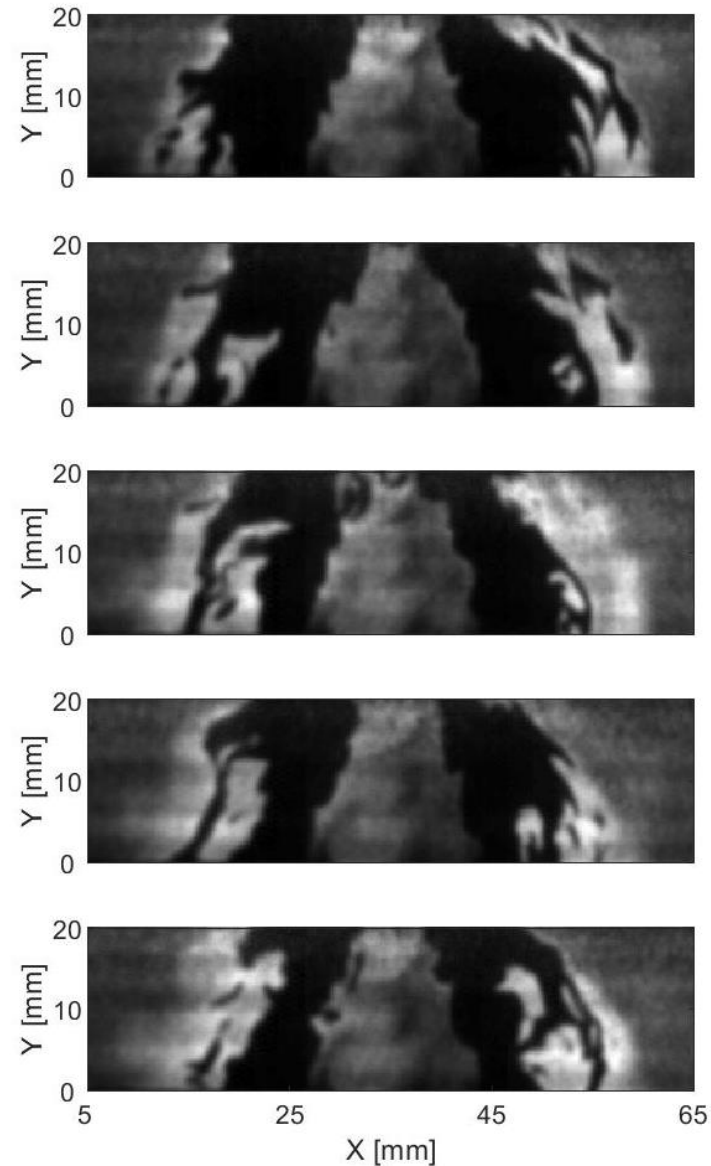
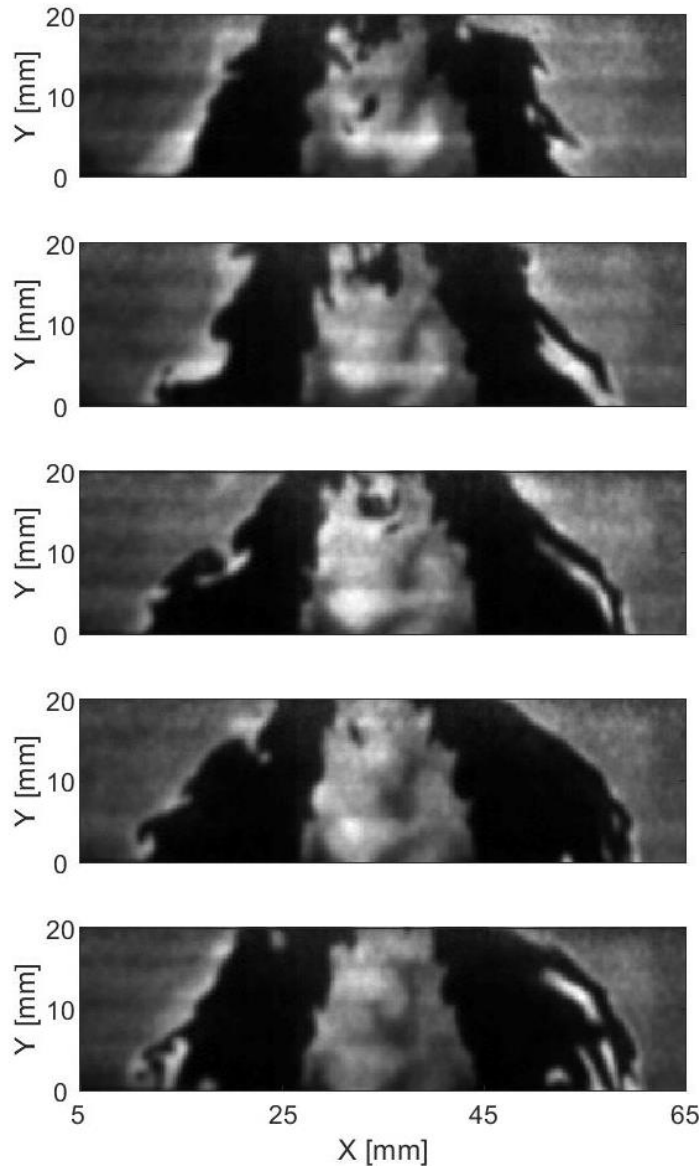
$$\varphi_{\text{outer}} = 0.70, \varphi_{\text{middle}} = 0.86$$
$$\varphi_{\text{overall}} = 0.73$$

Samarasinghe, J., et al. (2017) "The Effect of Fuel Staging on the Structure and Instability Characteristics of Swirl-Stabilized Flames in a Lean Premixed Multinozzle Can Combustor," *Journal of Engineering for Gas Turbines and Power*, **139**(12), pg. 121504

We considered three cases: unstable, center-nozzle staged, and right-nozzle staged, two nozzles with different efficacy

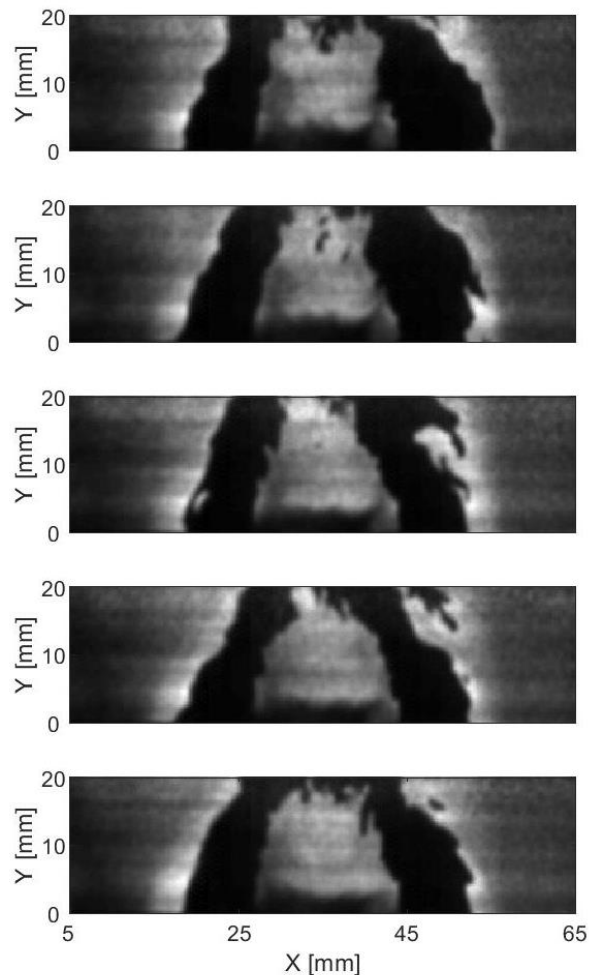


The unstable case displayed significant flame oscillations, where the adjacent branches oscillated in-phase

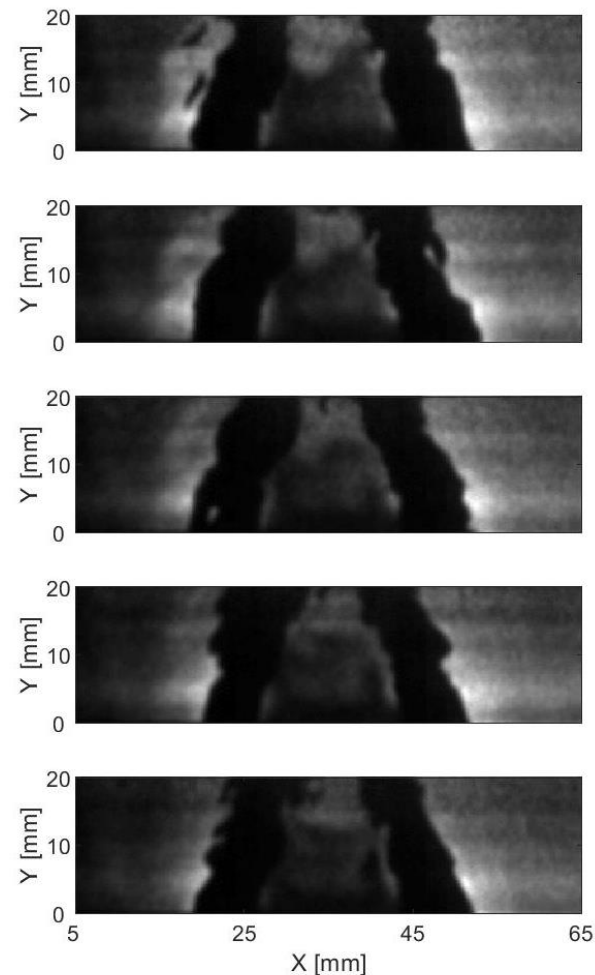


Center nozzle staging showed almost no oscillations, while
Nozzle 1 staging still had some coherent oscillations

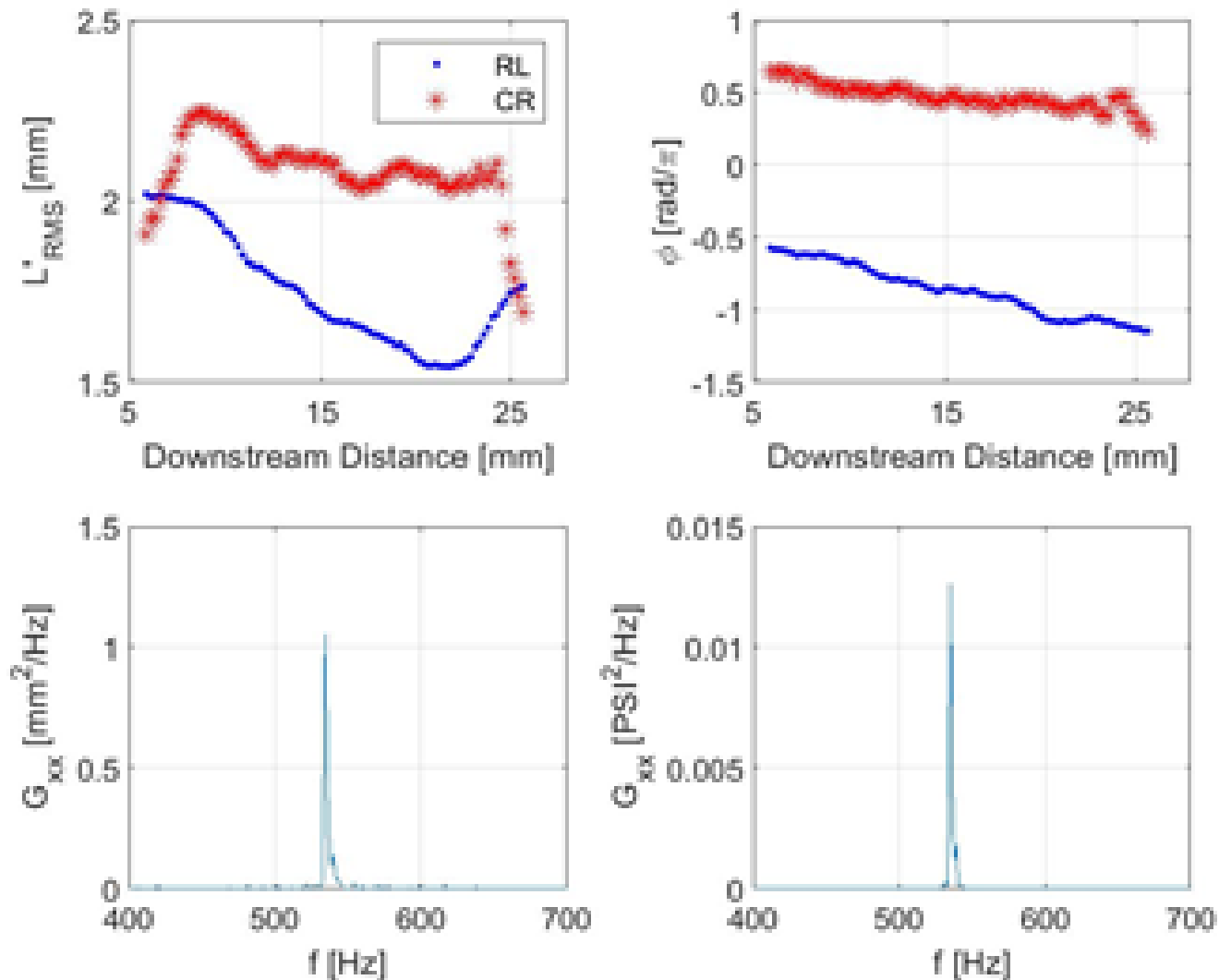
Nozzle 1 Staging



Center Staging



We quantify the flame branch oscillations using the lateral movement of the flame and the phase between the branches



Overview of presentation

- Project motivation and approach
- Review of previous results
- Year 3 major results:
 - Stability bifurcation during long-duration transients
 - Damping quantification
 - Local flame dynamics
- Conclusions and next steps

Wrap-up and Questions

— Key findings to date

- Implemented a number of new quantification metrics for stability in multi-nozzle combustors
- Quantified the impact of transient timescales on combustor behavior for multi- and single-nozzle combustors
- Began investigating local flame oscillations as a way to understand the effects of staging and flame dynamics in multi-nozzle systems

— Next steps

- Understand the role of intermittency in the dynamics of transient systems – need to quantify it as well
- Sensitivity of flame behavior to fuel composition with blends of natural gas + hydrogen

Acknowledgements

- **Penn State:** Dom Santavicca, Bryan Quay, Janith Samarasinghe, Wyatt Culler, Dan Doleiden, Adam Howie, John Strollo, Xiaoling Chen, Jackson Lee, Steve Peluso, Ankit Tyagi, Olivia Sekulich
- **GE Global Research:** Keith McManus, Tony Dean, Janith Samarasinghe, Fei Han
- **DOE/NETL:** Mark Freeman
- College of Engineering Instrumentation Grant Program, Mechanical and Nuclear Engineering at Penn State

Questions?

Understanding Transient Combustion Phenomena in Low-NO_x Gas Turbines

Project DE-FE0025495, Oct. 2015 – Sept. 2018

Program Monitor: Mark Freeman

PI: Jacqueline O'Connor, Ph.D.

Co-PI: Dom Santavicca, Ph.D.

RE: Stephen Peluso, Ph.D.

Graduate students: Wyatt Culler, Dan Doleiden, Adam Howie, John Strollo

Undergraduates: Olivia Sekulich

Industry Partner: GE Global Research
Keith McManus, Tony Dean, Fei Han

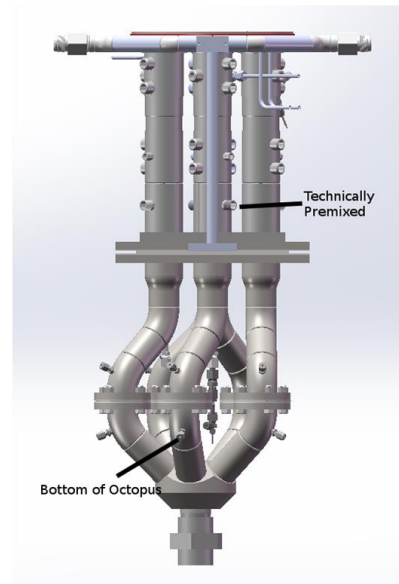
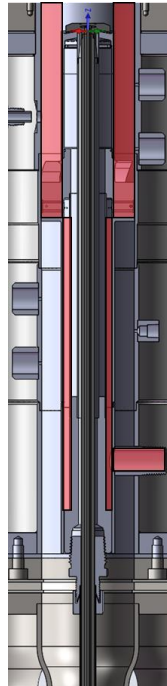
Mechanical and Nuclear Engineering
Pennsylvania State University
sites.psu.edu/rfdl/



Backup slides

The convective time depends on the amount of additional fuel added.

Center Staging	Calculated Convective Time
0.75	75 ms
0.80	37 ms
0.85	25 ms



A general logistic regression is used to obtain the time constants.

Used to model the growth (or decay) of systems that have a lower and upper asymptote

Growth is initially exponential before leveling off

Logistic fits are symmetric, but can be made general to change where the maximum growth rate is

Using a more general logistic regression:

$$P'(t) = \frac{A - B}{(1 + be^{k(t-t_0)})} + B$$

A: Instability Amplitude

B: Stable Amplitude

k : Logistic Rate (negative is growth, positive is decay)

t_0 : Time offset

b : Pre-exponential factor, typically taken as 1

A general logistic regression is used to obtain the time constants.

Original Equation: $P'(t) = \frac{A-B}{(1+e^{k(t-t_0)})} + B$

Fractional Amplitude Characteristic Time:

$$\frac{A-B}{R} = \frac{A-B}{(1+e^{k(t-t_0)})} + B$$

R is the amplitude fraction

Solving for $(t - t_0)$

$$(t - t_0) = \ln \left(\left(R + \frac{B}{A-B} - 1 \right) \right) \left(\frac{1}{k} \right)$$

The absolute value of this should be proportional to a time constant

This will not be dependent on valve actuation time

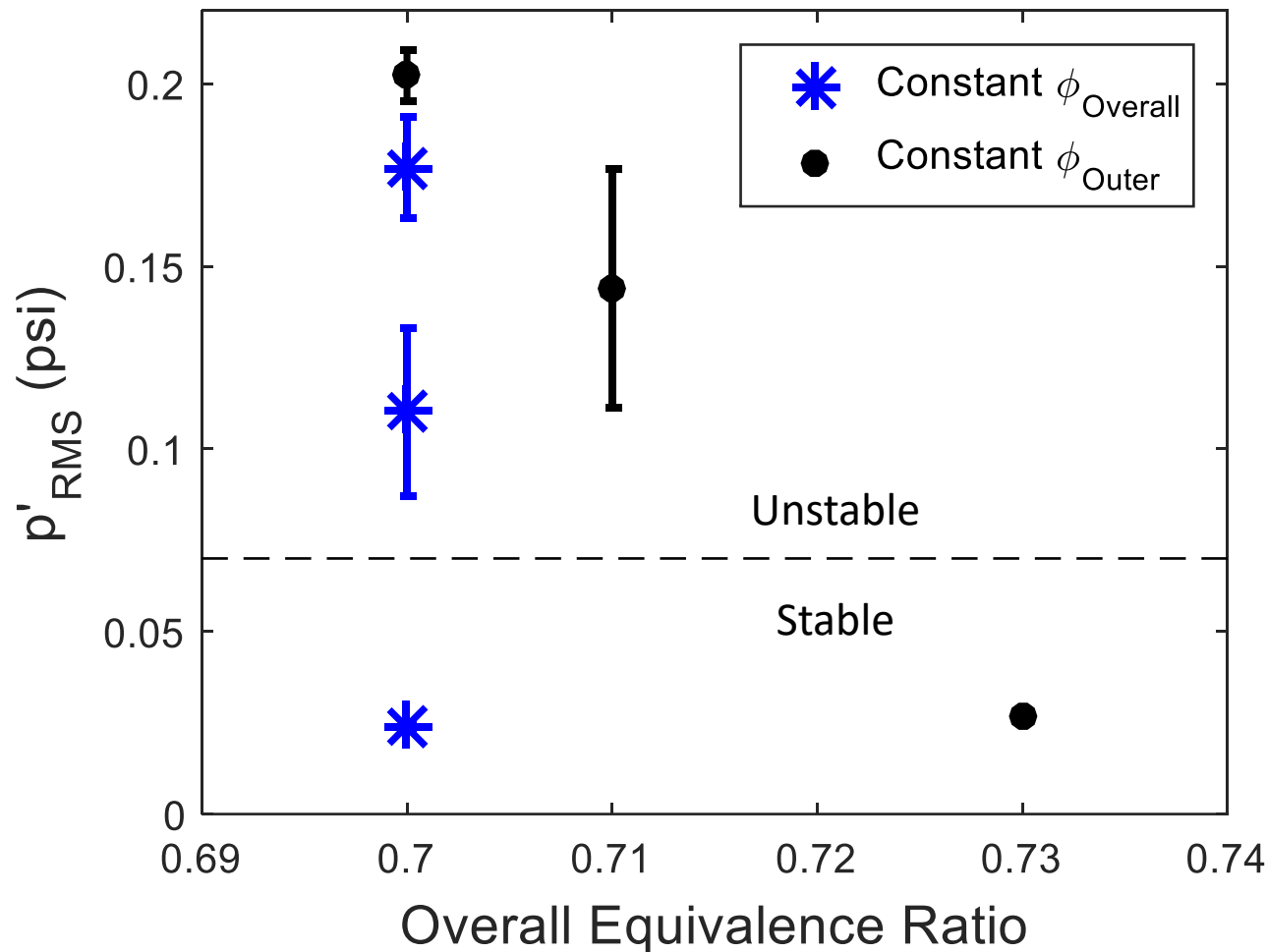
Half-Maximum Time for $b=1$ (neglecting zero offset B)

Given by t_0 :

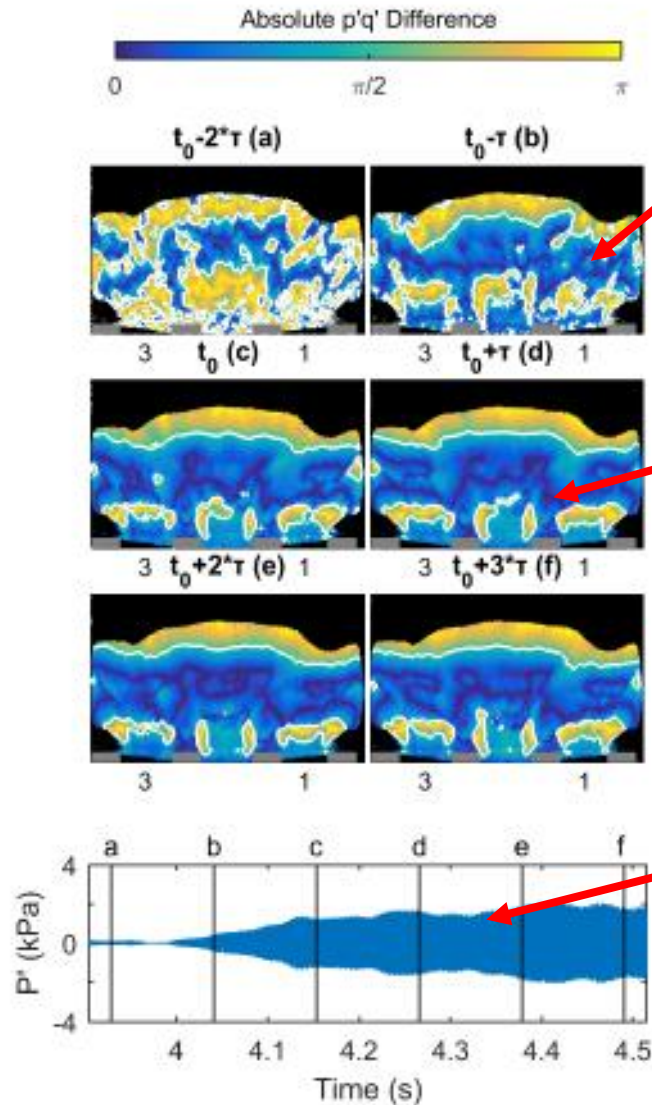
$$P(t_0) = \frac{A-B}{1+e^{k(t_0-t_0)}} = \frac{(A-B)}{2}$$

Will depend on valve actuation time

Both staging strategies, i.e. increasing overall equivalence ratio and keeping overall equivalence ratio constant resulted in successfully suppressing instabilities



Differences in staging efficacy near the bifurcation point typically relate back to the level of intermittency



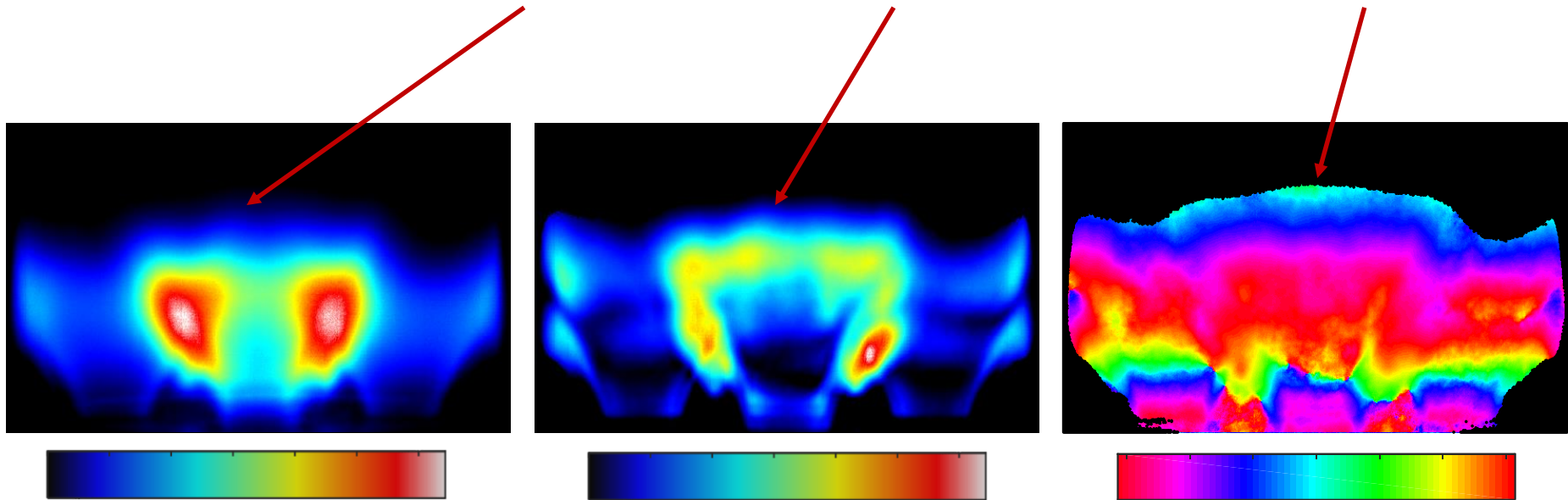
Sharp transition to coherent phase relationship

In-phase relationship between heat release rate oscillations and pressure

Continued, but somewhat intermittent, growth in instability amplitude after coherence switch

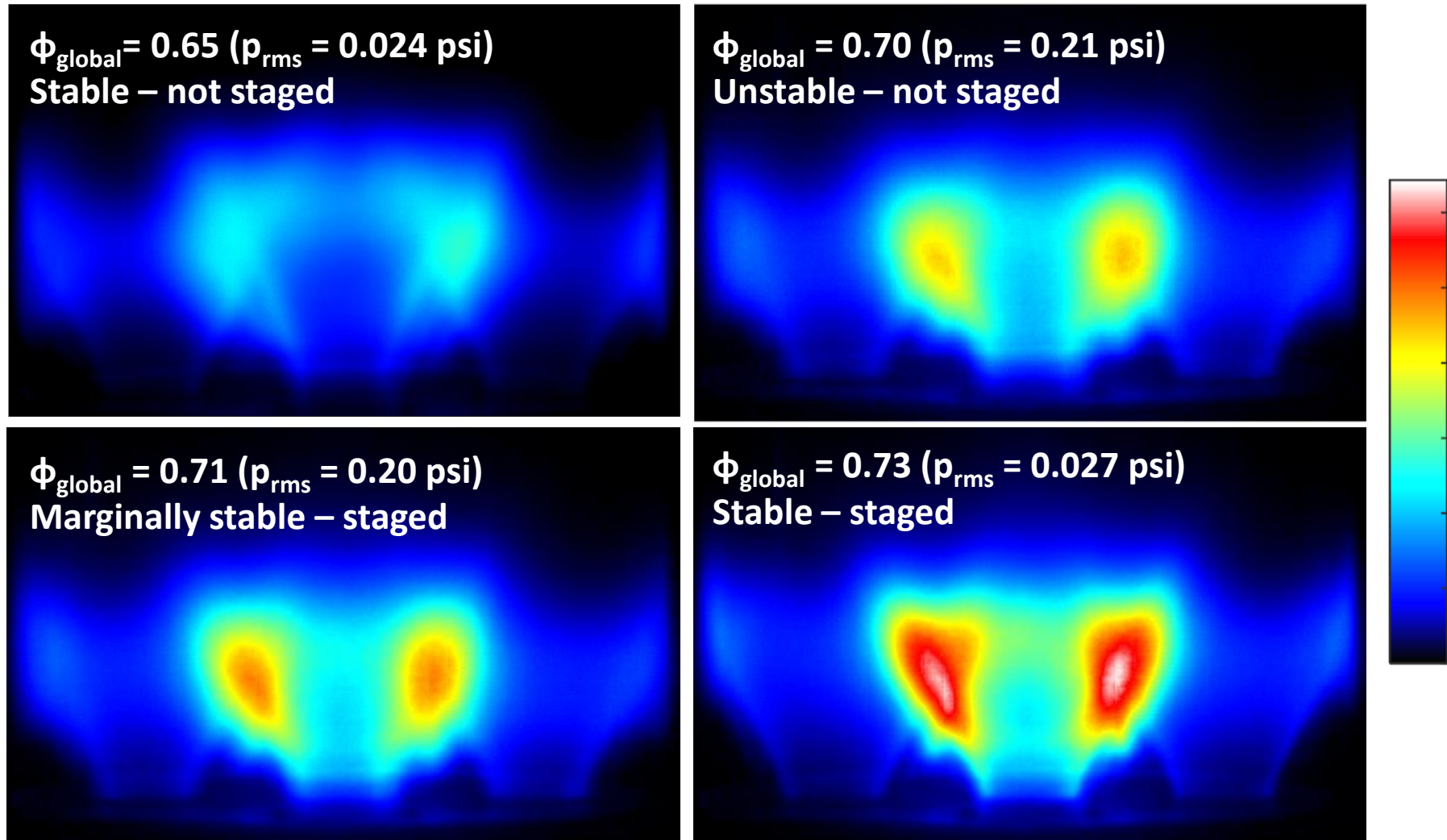
Images of forced flames can be decomposed into mean, RMS and phase components to understand instability mechanisms

$$\text{Filtered Image} = \text{Mean Image} + \sqrt{2} * \text{RMS Image} * \cos(2\pi ft + \text{Phase Image})$$

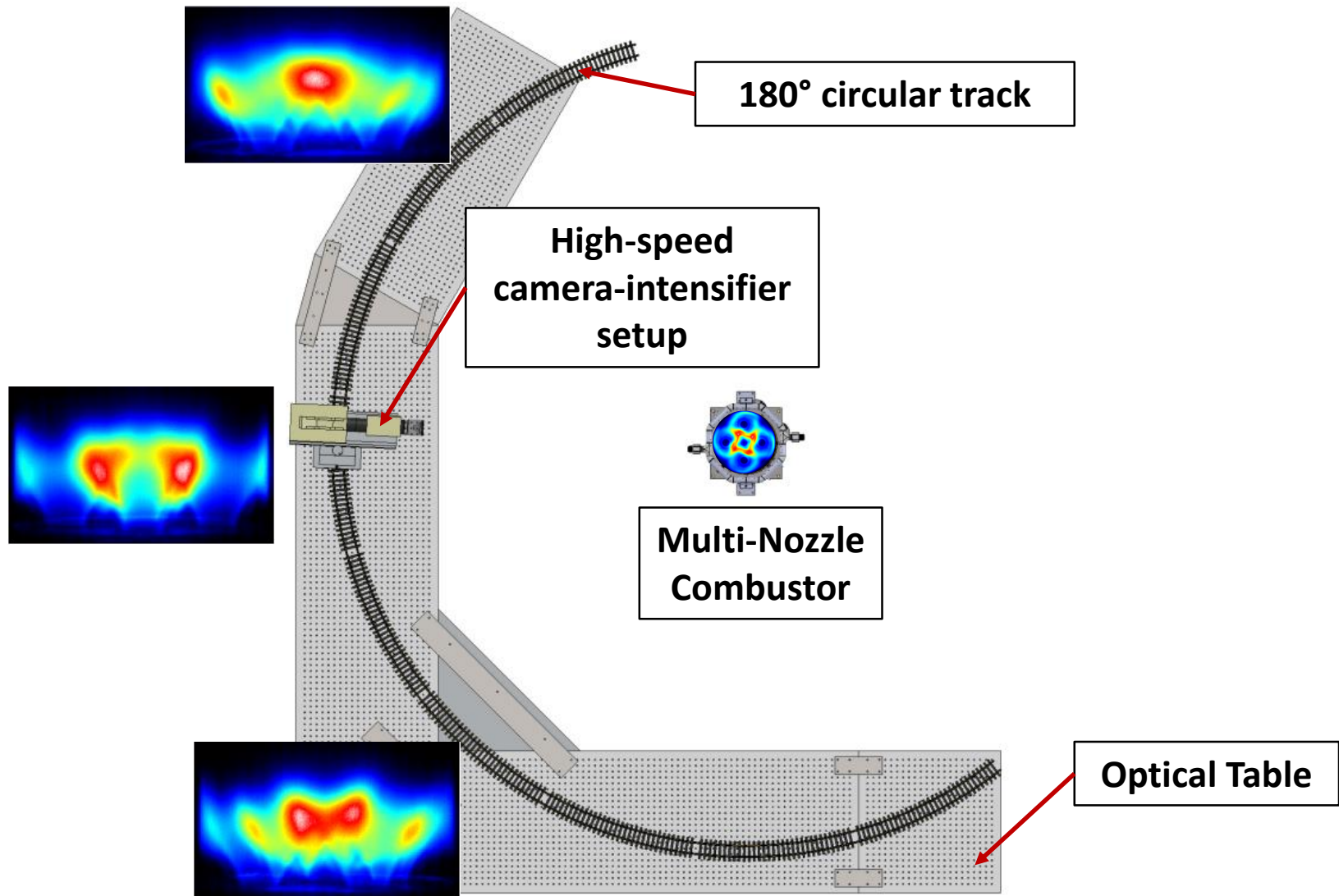


Mean, RMS, and phase images are analyzed at different test conditions to determine the effects of fuel staging on time-averaged and phase-averaged flame structure

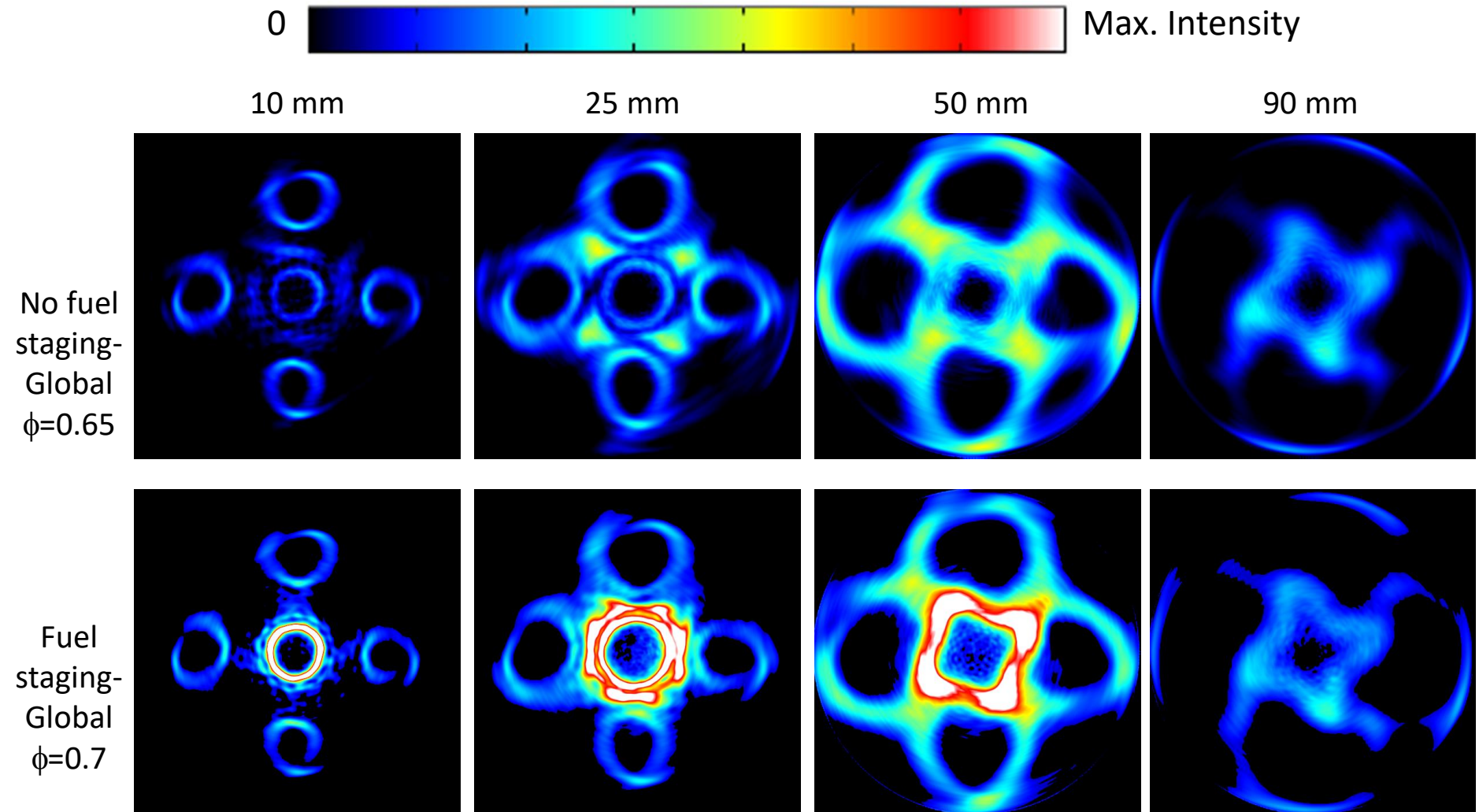
Flame structure does not change significantly with additional staging, though center flame has higher heat release



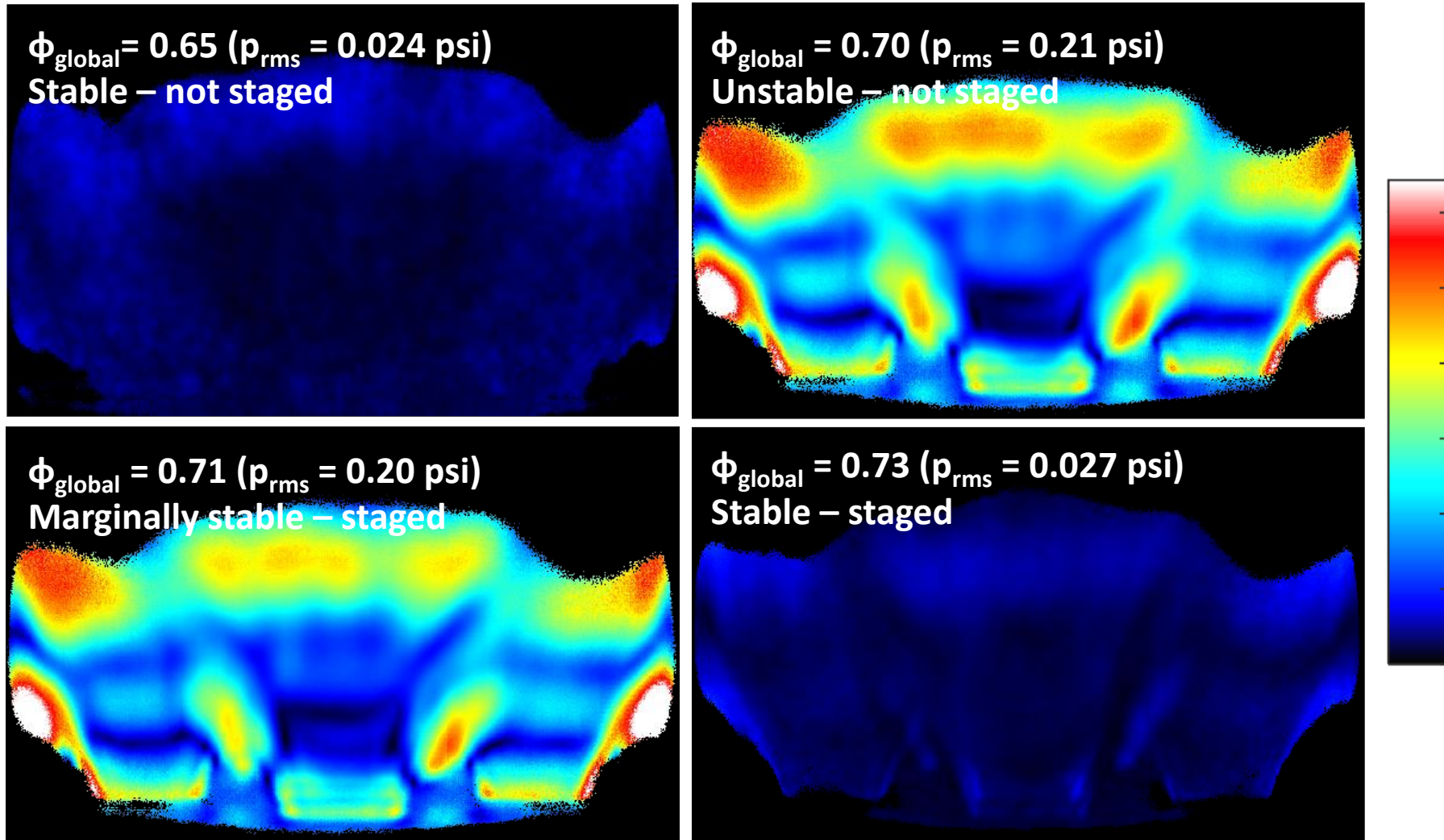
Line-of-sight chemiluminescence images are acquired at 5° increments around the combustor to create tomographic image



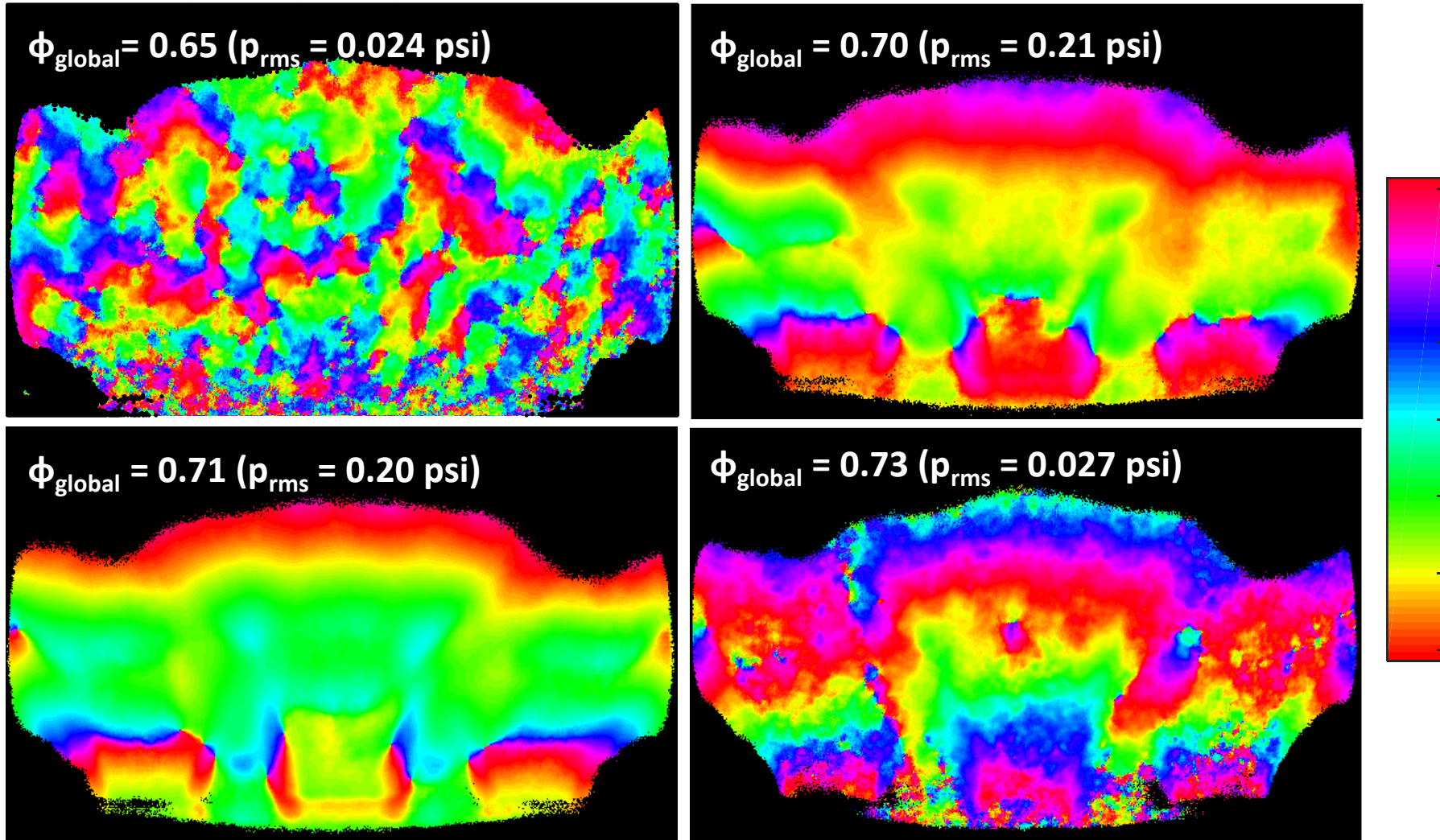
Different flame structures are observed between stable unstaged and stable staged cases through tomographic imaging



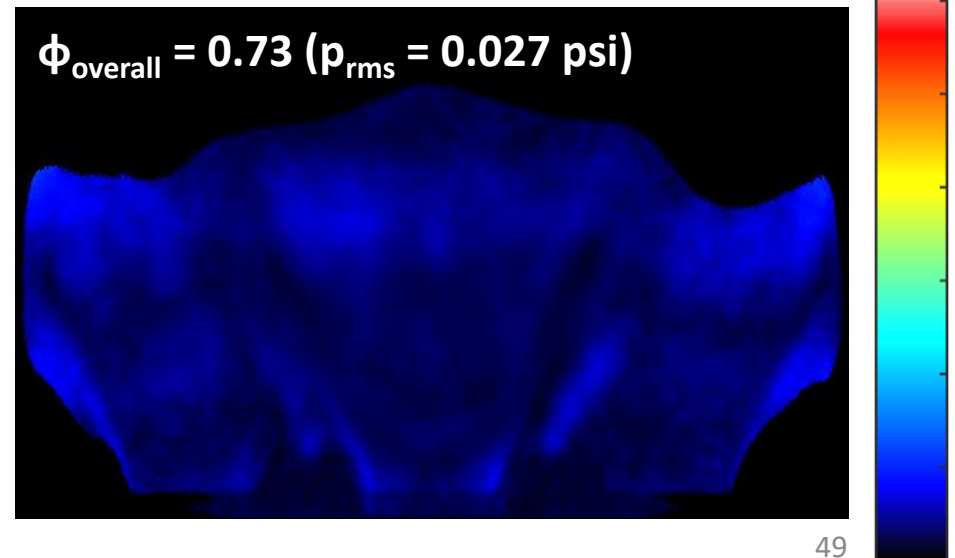
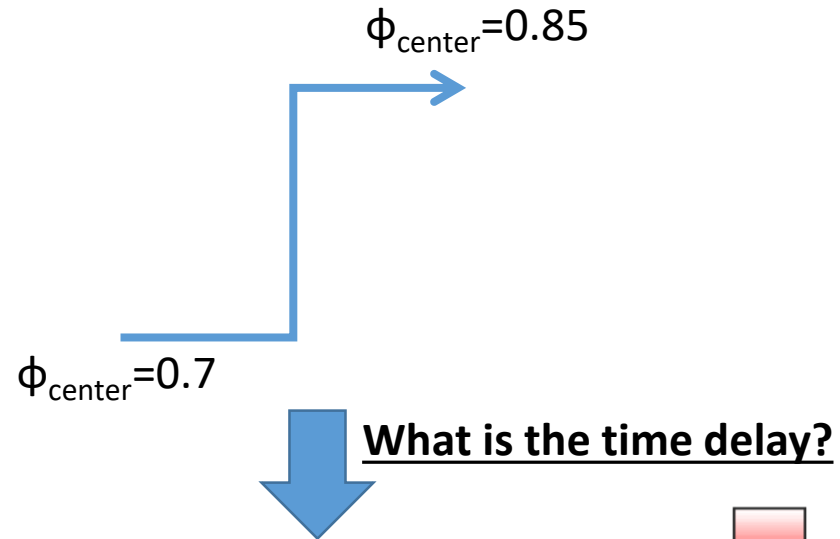
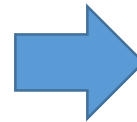
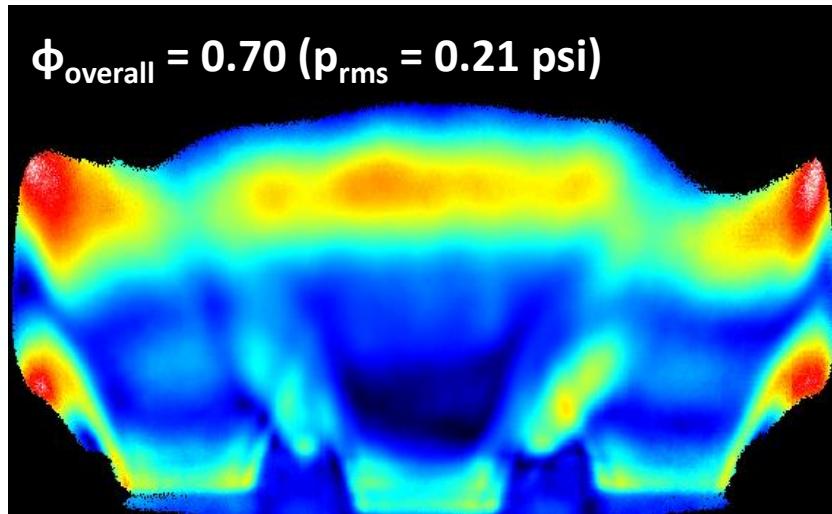
Heat release rate RMS levels are suppressed with staging, though signature is visible even at highest staging amount



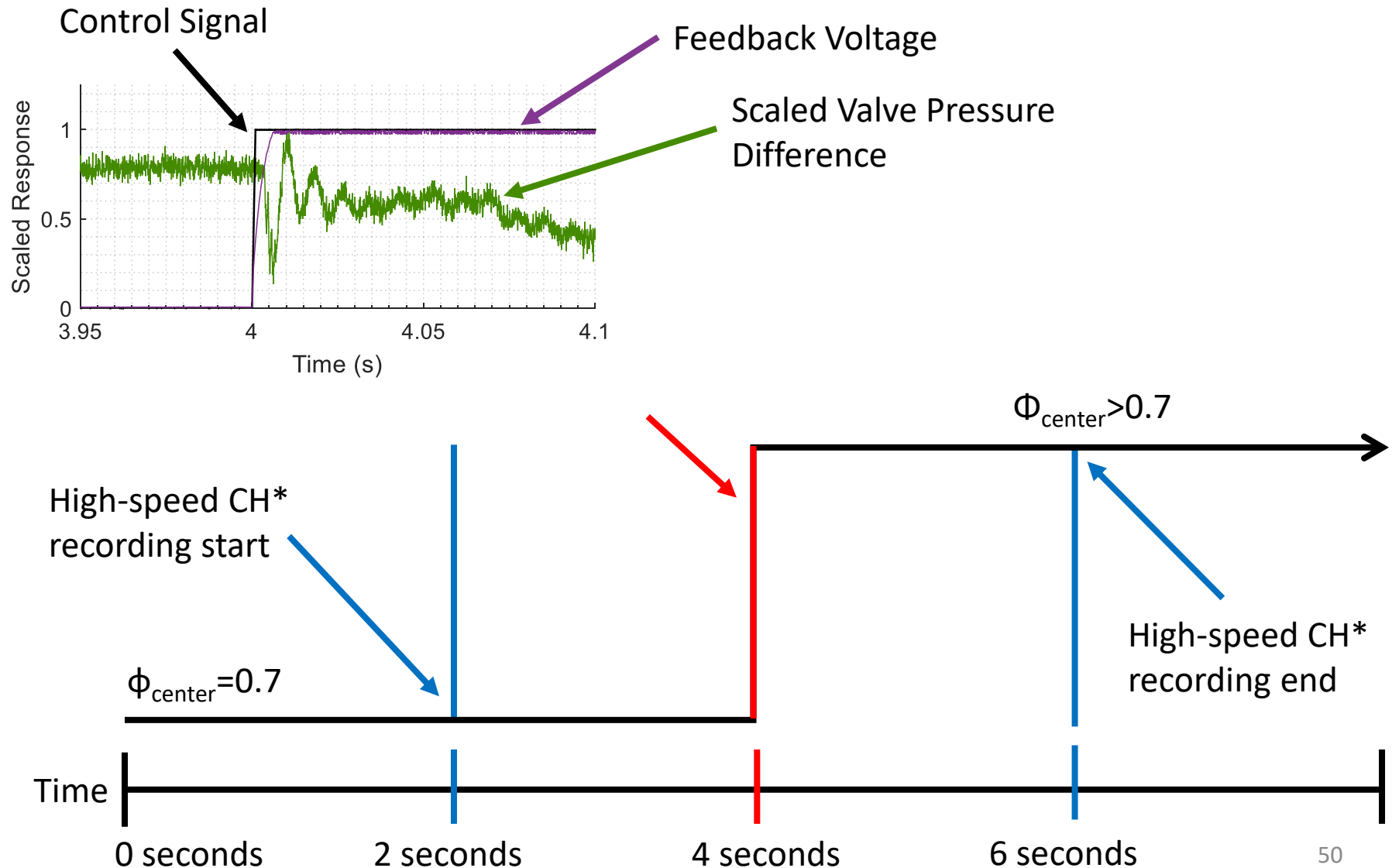
Phase of oscillations seems to indicate phase shift in oscillations during staging, possible suppression mechanism



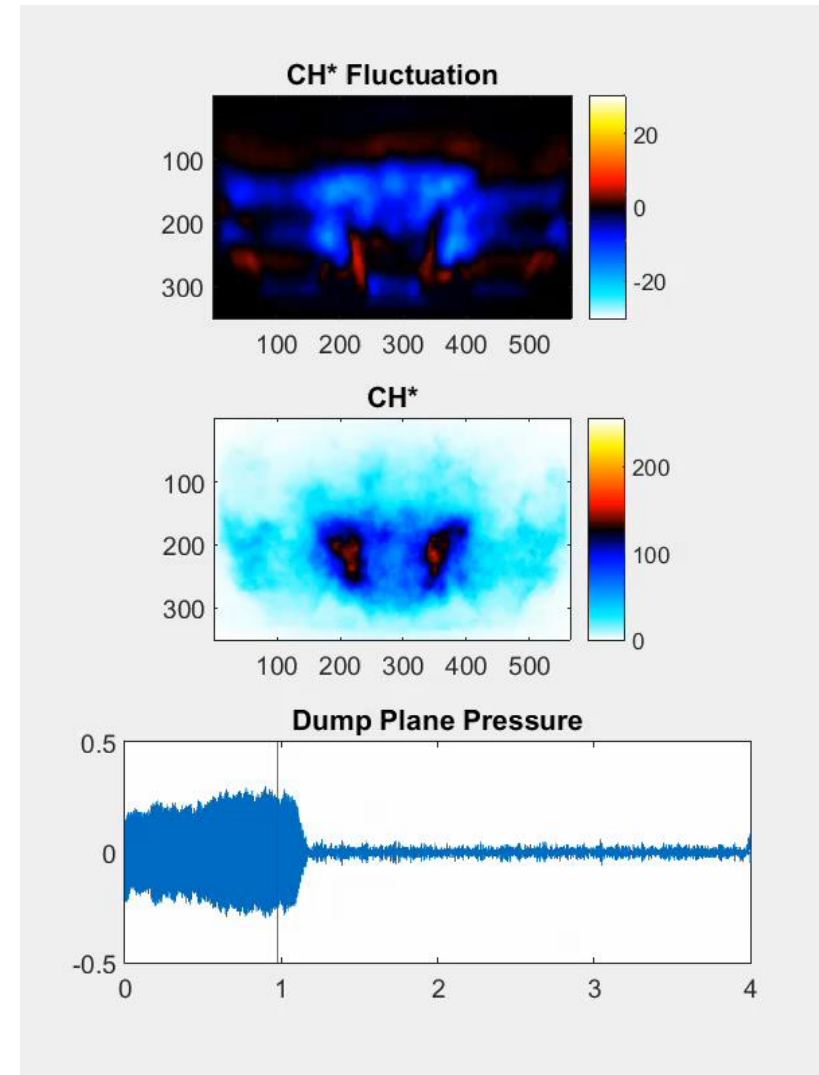
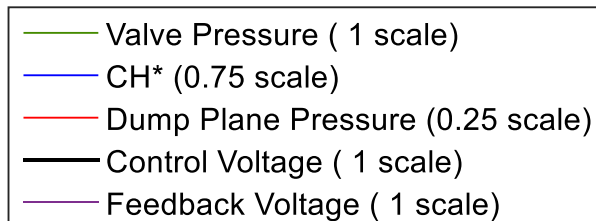
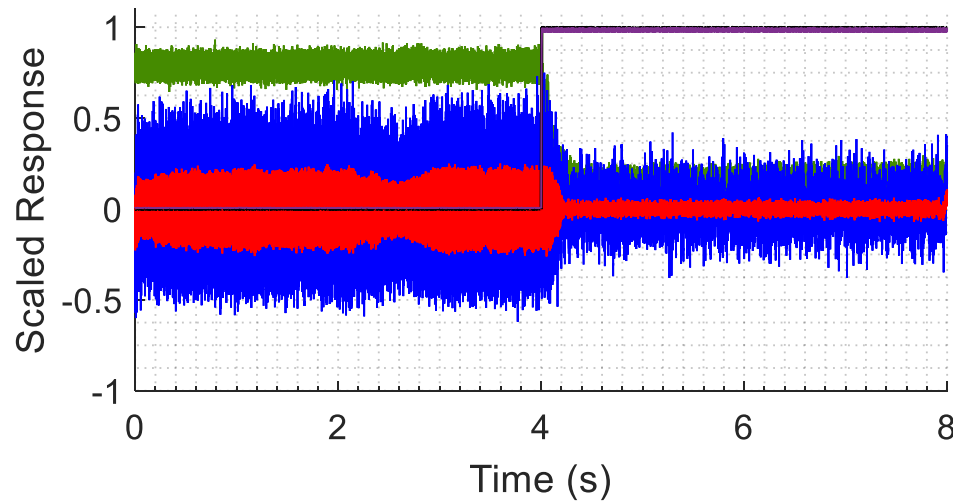
Task 4: Test matrix for initial transient testing considers step-change transients to determine natural time-scales of system



Impulse transients are executed using a fast-acting proportional control valve



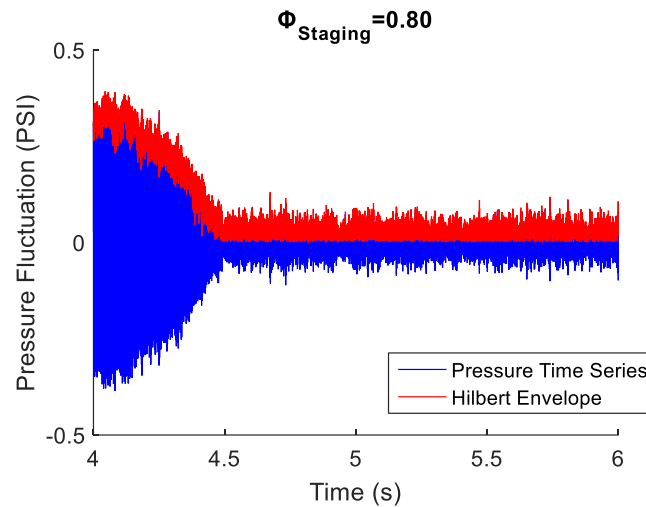
Both the fluctuation in CH^* (blue) and pressure (red) track each other through the transient event.



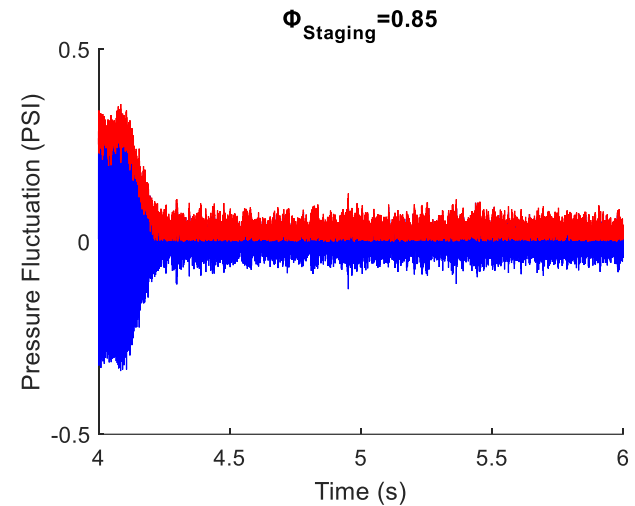
The growth/decay time of the instability reflects a natural time-scale of the system, and is dependent on staging level

Unstable →
Stable

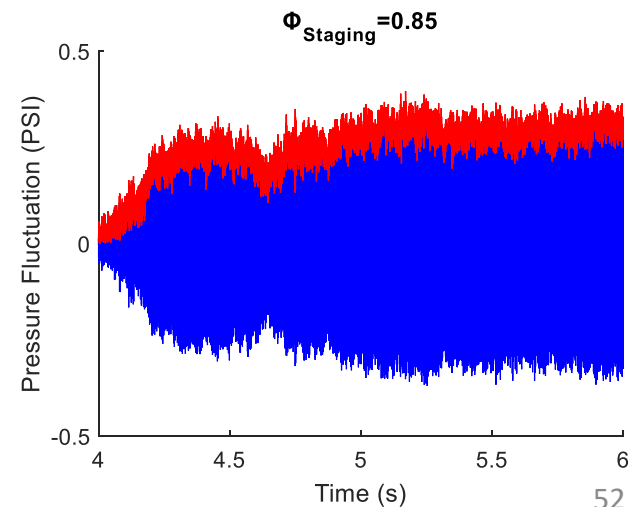
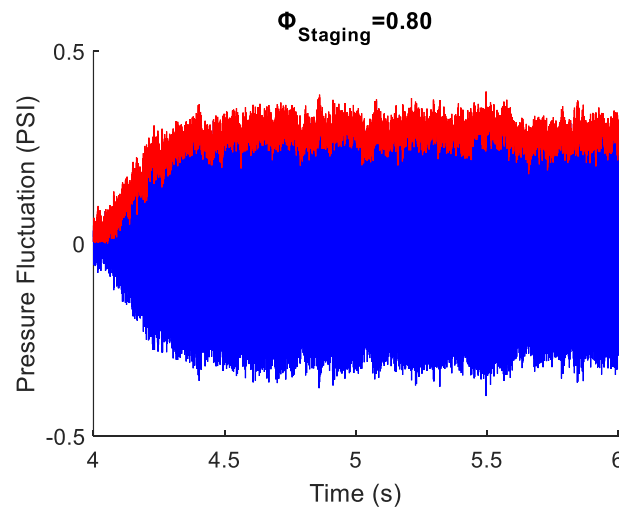
Center-nozzle: $\phi=0.8$



Center-nozzle: $\phi=0.85$



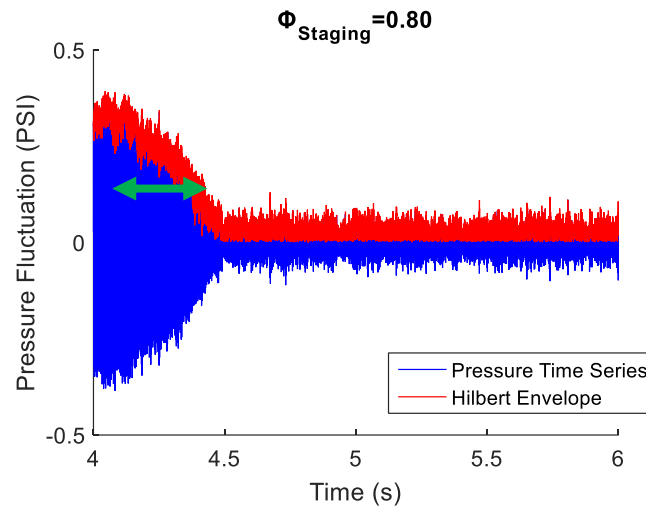
Stable →
Unstable



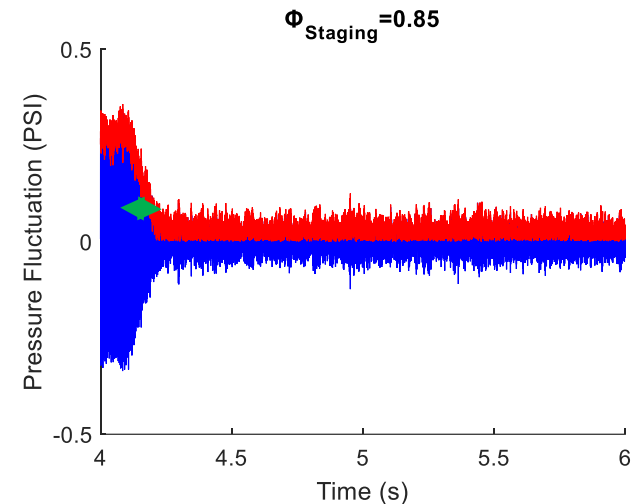
The growth/decay time of the instability reflects a natural time-scale of the system, and is dependent on staging level

Unstable →
Stable

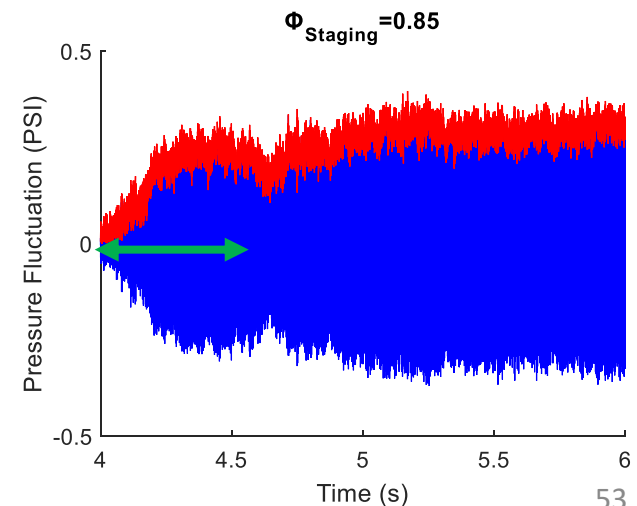
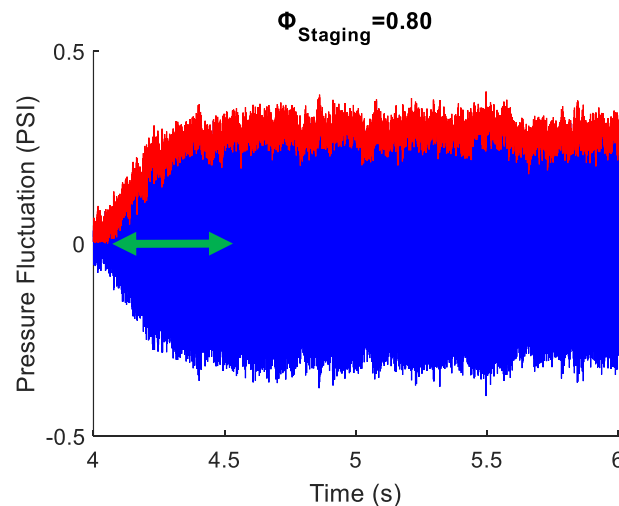
Center-nozzle: $\phi=0.8$



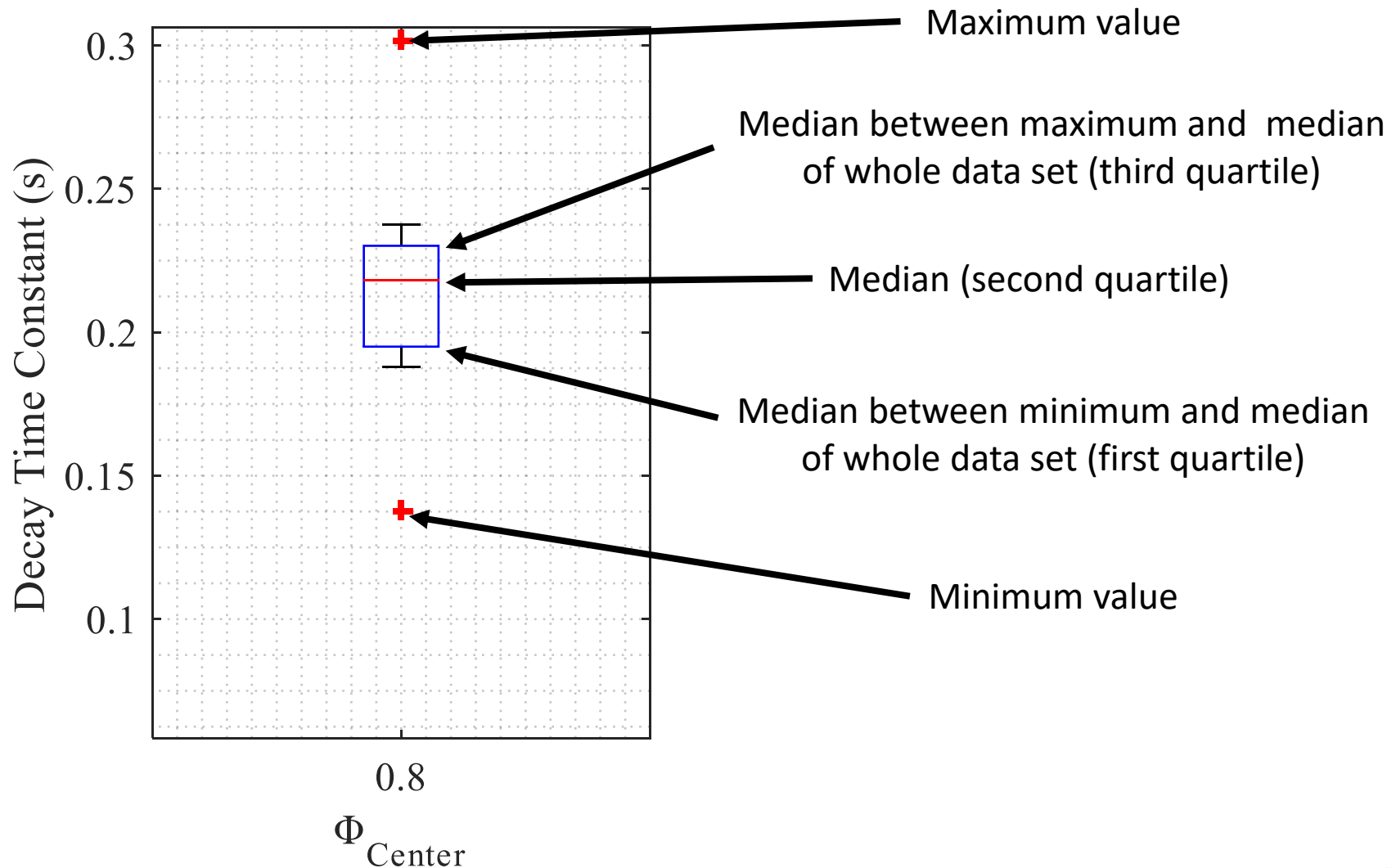
Center-nozzle: $\phi=0.85$



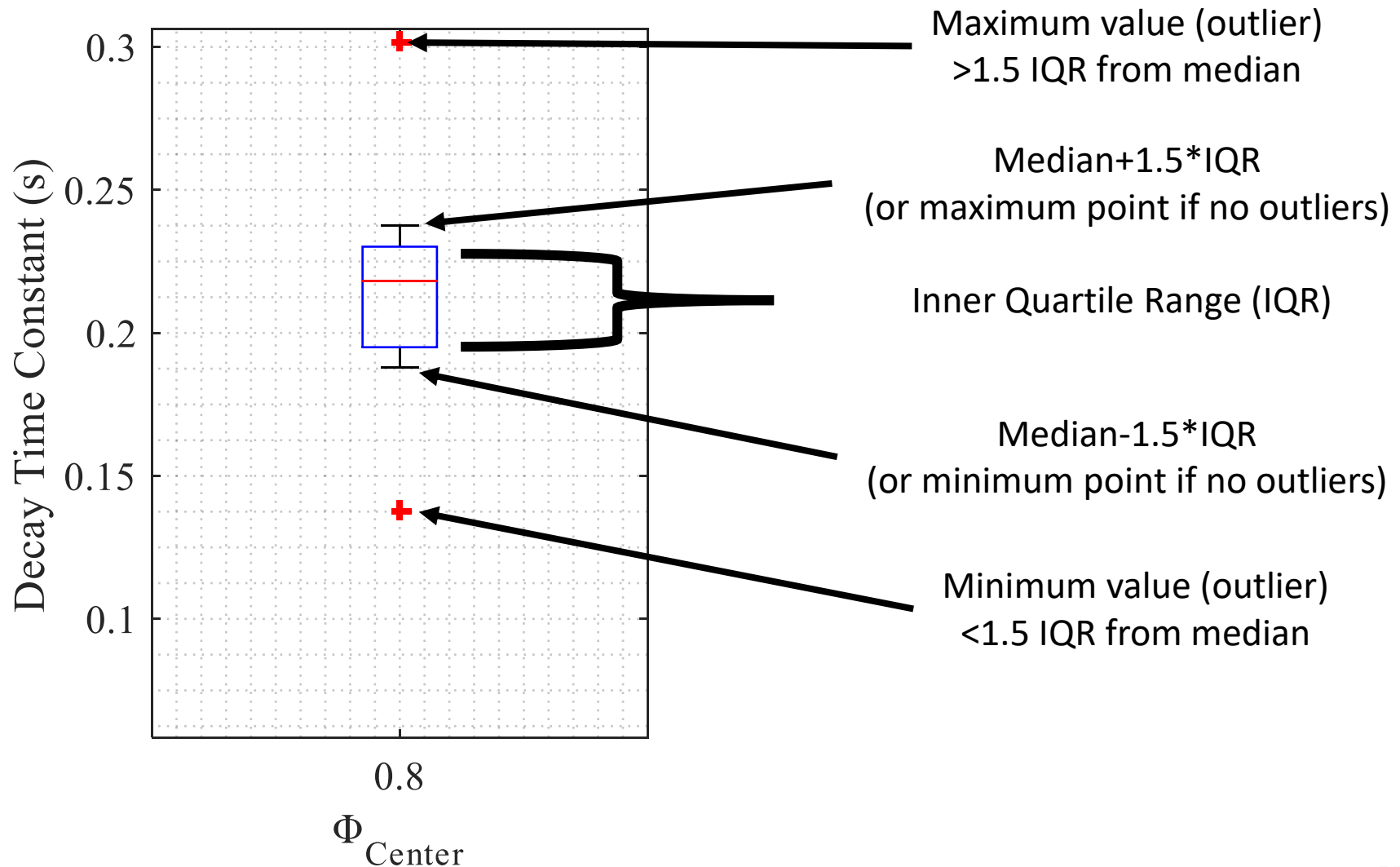
Stable →
Unstable



Box-and-whisker plots provide a useful way to visualize ensemble data.

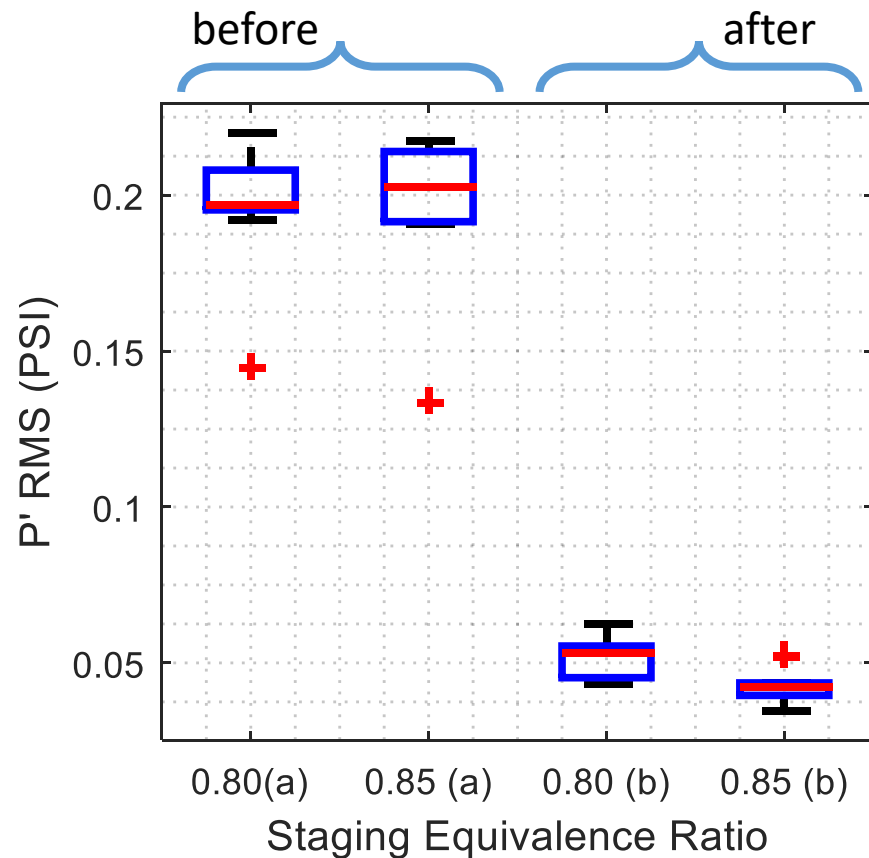


Box-and-whisker plots provide a useful way to visualize ensemble data.

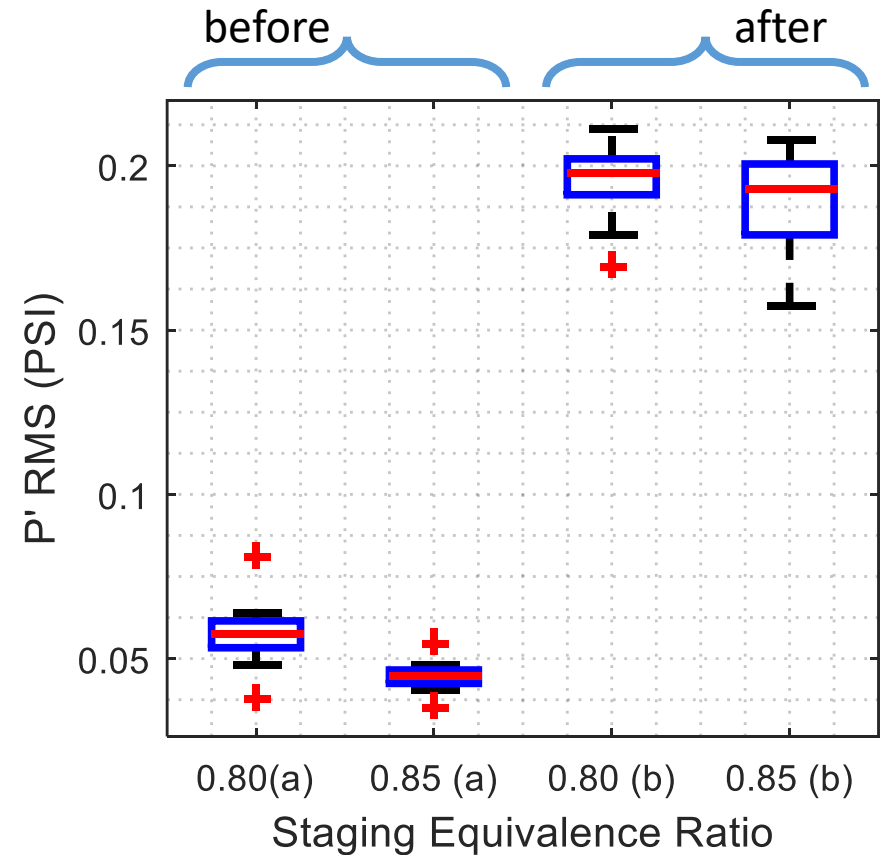


The pressures before and after the transient mirror the steady-state test results, showing high repeatability

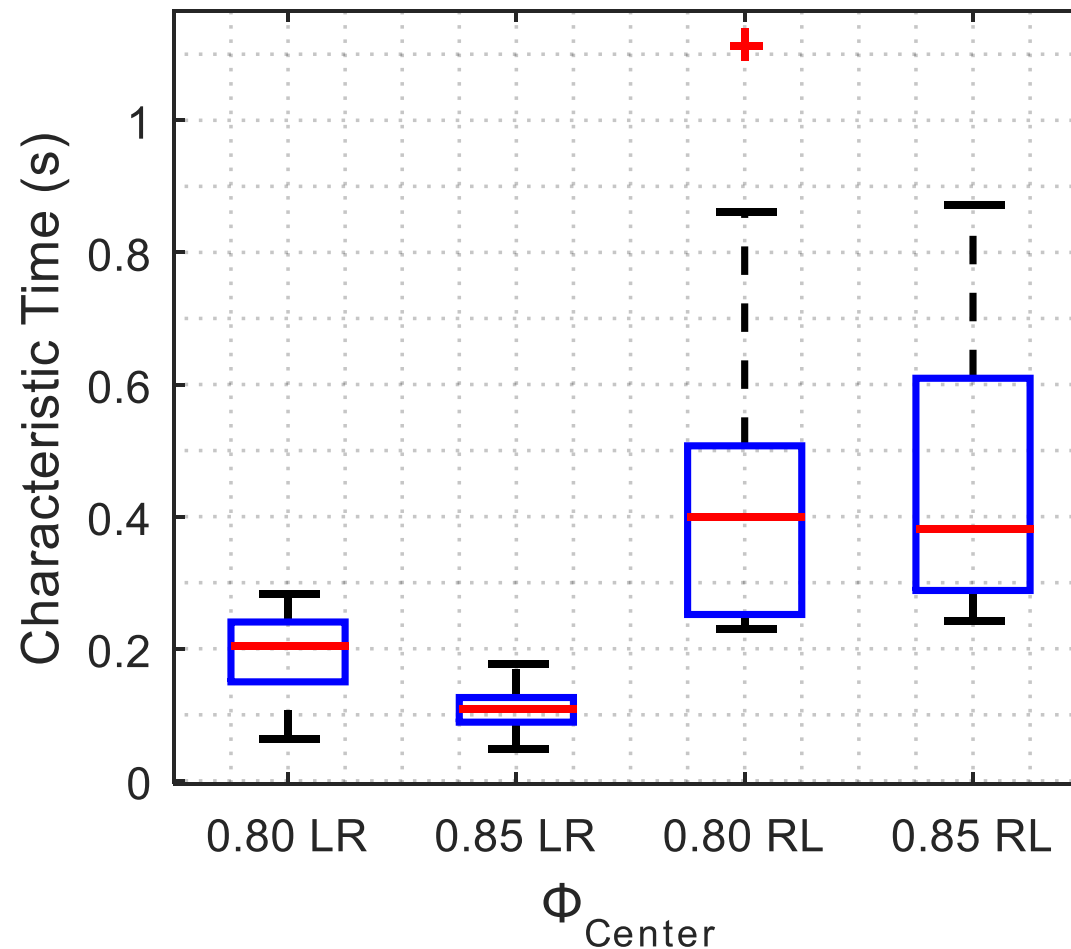
Unstable to Stable



Stable to Unstable

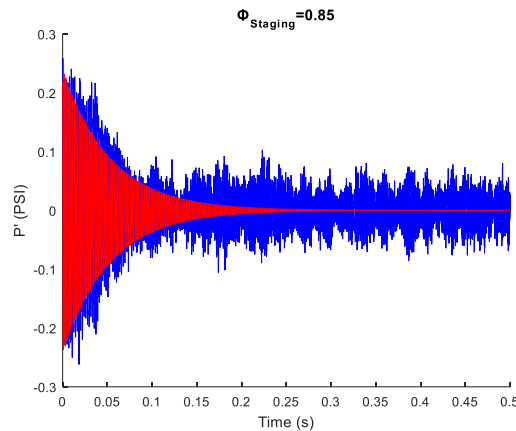


The characteristic decay time depends on staging amplitude, but the characteristic rise time does not appear to

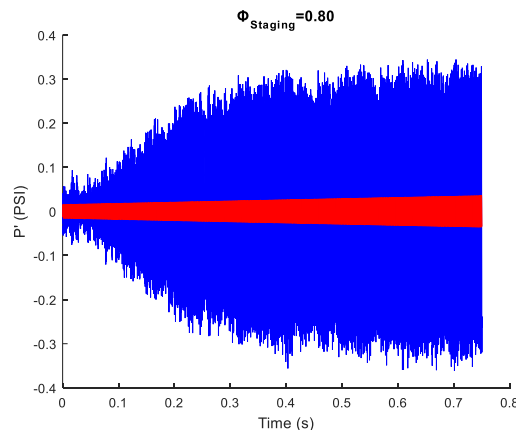


The functional form of the growth and decay profiles can help illuminate some of the physics involved in the processes

Model 1: Damped linear oscillator decaying at a single frequency



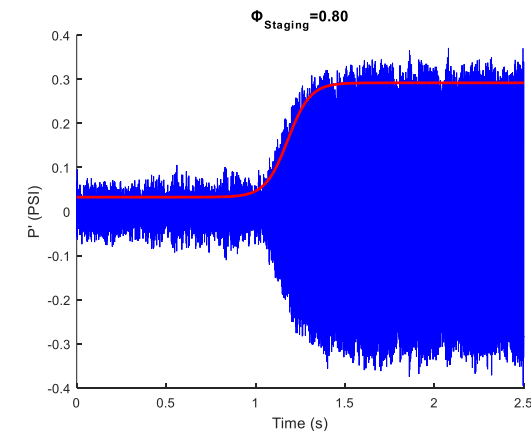
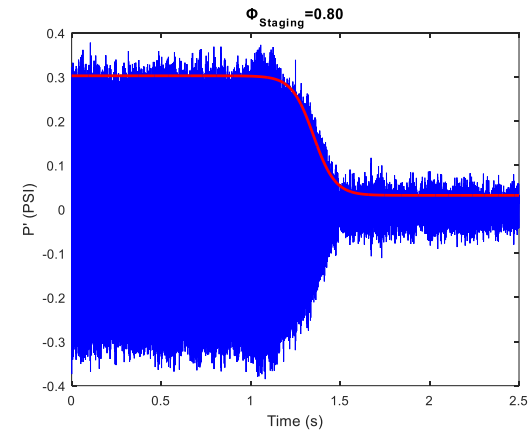
$$P'(t) = Ae^{-\lambda t} + AB * (1 - e^{-\lambda t}) * \sin(\omega t + \Phi)$$



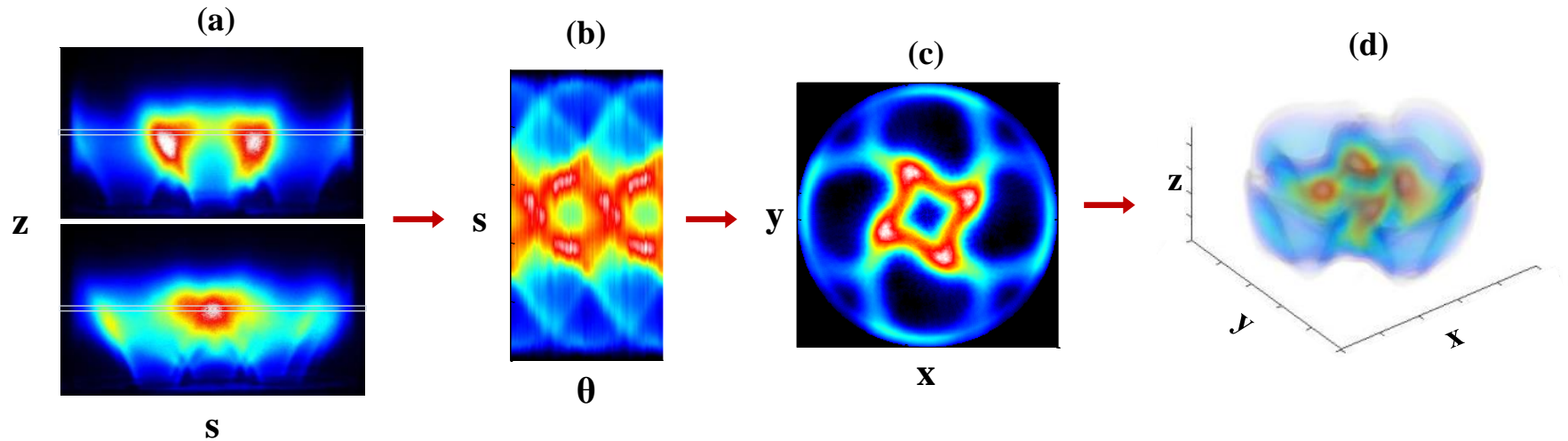
$$P'(t) = AB e^{-\lambda t} + B * (1 - e^{-\lambda t}) * \sin(\omega t + \Phi)$$

Model 2: General Logistic Growth/Decay

$$P'(t) = \frac{A - B}{(1 + e^{k(t-t_0)})} + B$$

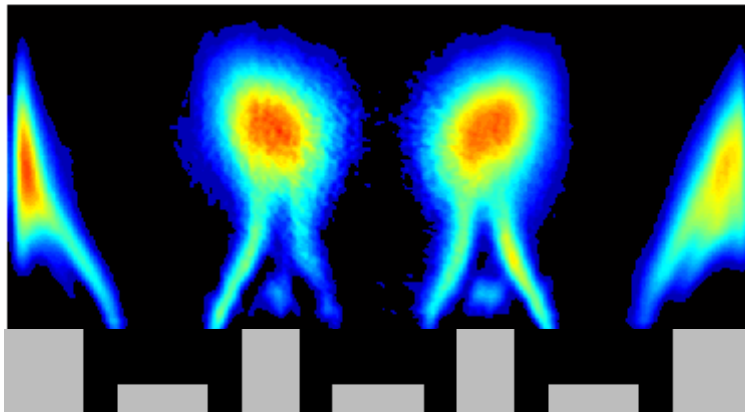


A tomographic reconstruction technique is used to obtain the 3-D chemiluminescence distribution

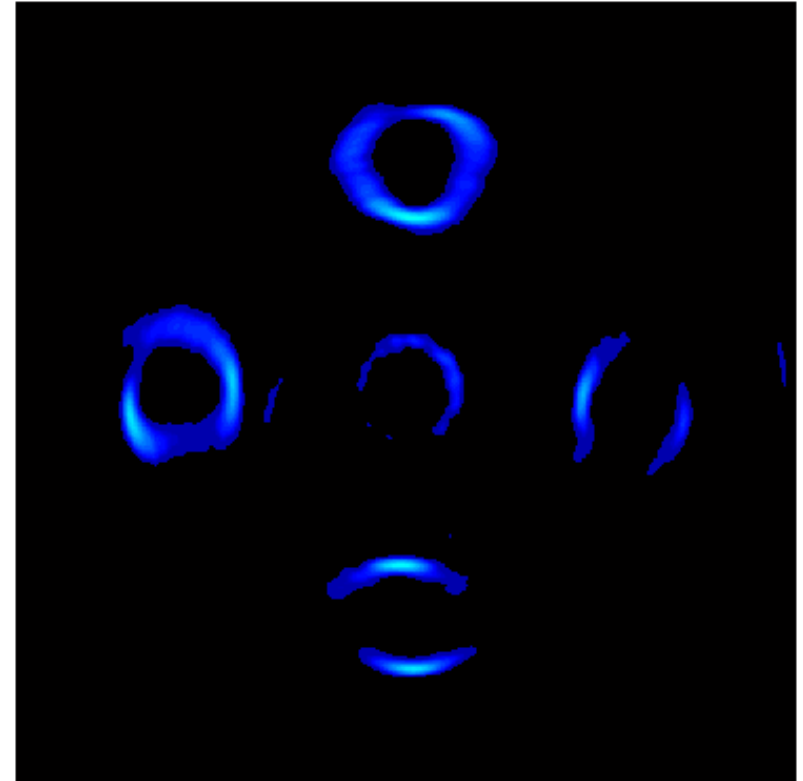


- (a) Each line-of-sight image is divided into pixel wide horizontal bins
- (b) The horizontal bins from each image acquired around the combustor are combined into an array
- (c) This array is input into a filtered backprojection algorithm which reconstructs a 2-D cross section of the flame
- (d) The cross sections at every axial location are stacked to obtain a 3-D matrix of the flame's chemiluminescence distribution

Horizontal 2-D slices of the 3-D image illustrate the flame structure at different points downstream of the dump plane



Location of slice

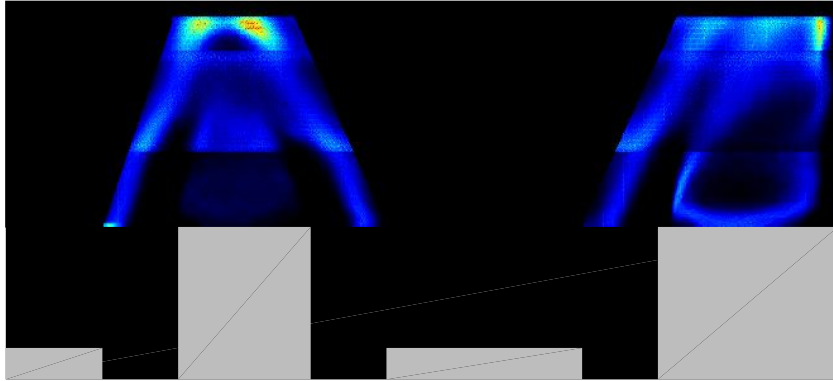


Horizontal slice

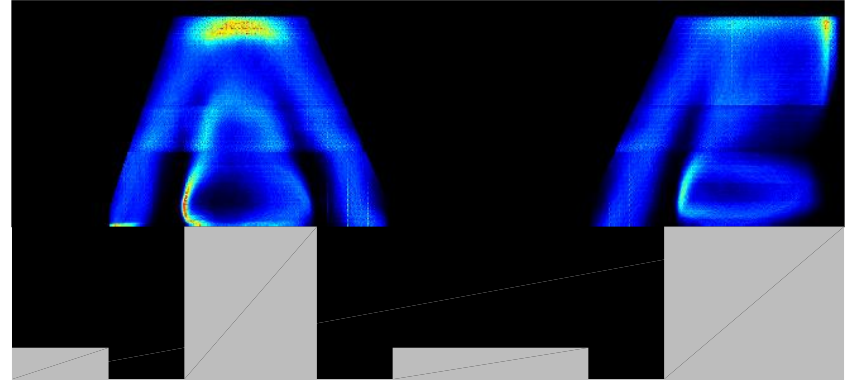
Low Intensity  High Intensity

Time-averaged FSD images

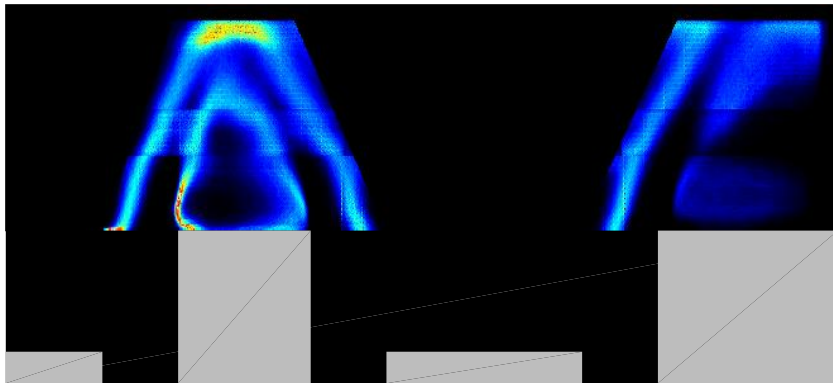
$\phi = 0.65$, all nozzles fueled equally



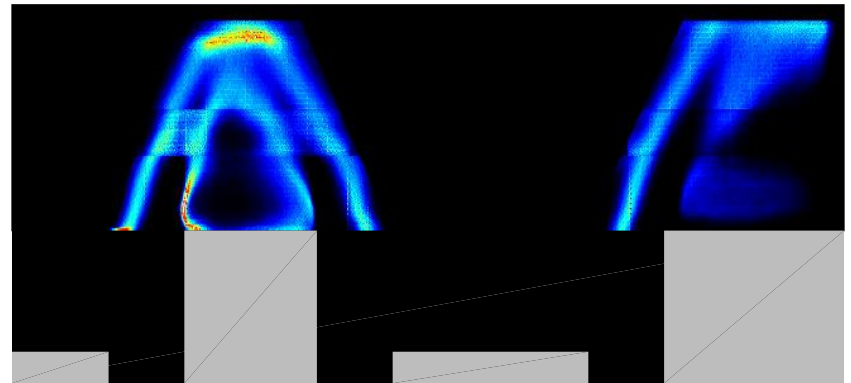
$\phi = 0.70$, all nozzles fueled equally



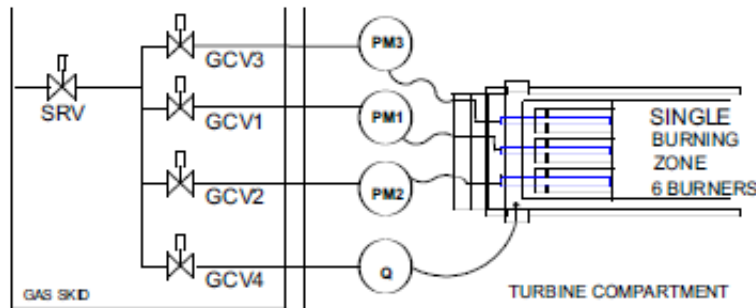
Staged - $\phi_{\text{outer}} = 0.67$, $\phi_{\text{middle}} = 0.82$



Staged - $\phi_{\text{outer}} = 0.70$, $\phi_{\text{middle}} = 0.85$

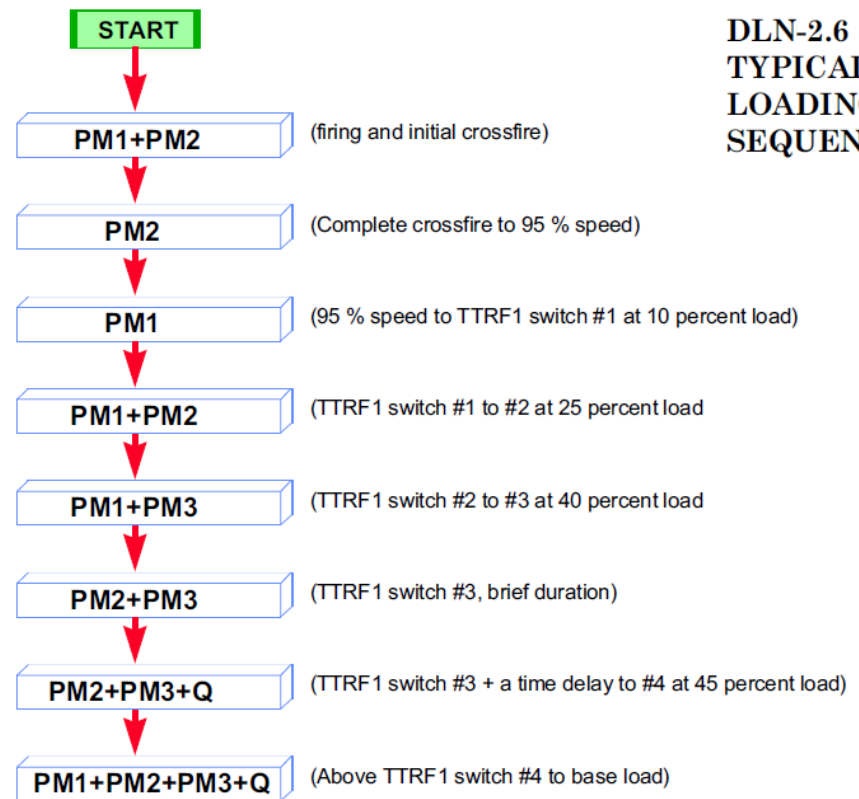
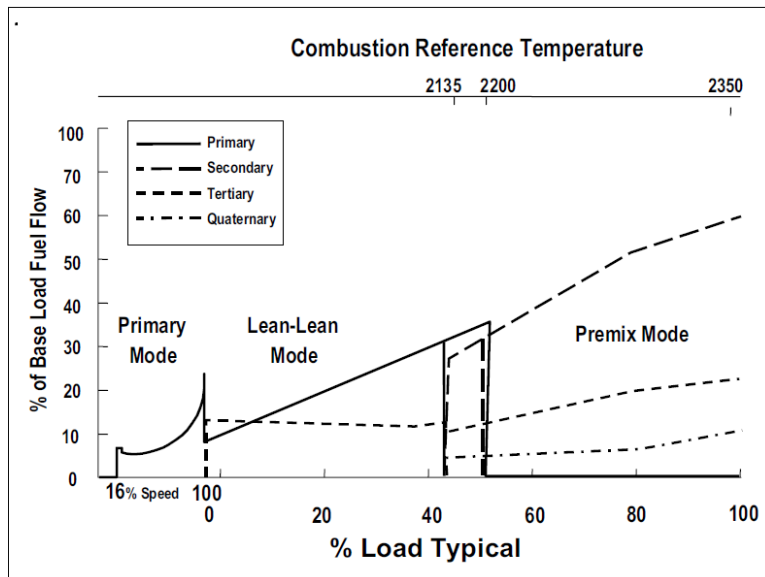


Engine load is typically varied by either varying fuel staging or the equivalence ratio of certain fuel nozzles



SRV SPEED/RATIO VALVE
GCV1 GAS CONTROL PM1
GCV2 GAS CONTROL PM2
GCV3 GAS CONTROL PM3
GCV4 GAS CONTROL Quaternary

PM3 - 3 NOZ. PRE-MIX ONLY
PM2 - 2 NOZ. PRE-MIX ONLY
PM1 - 1 NOZ. PRE-MIX ONLY
Q - QUAT MANIFOLD, CASING, PRE-MIX ONLY



Stability limits of certain operating points are already known, current work focuses on mapping instability with fuel splits

		U (m/s)						
		15.5	18.1	20.7	23.3	25.8	28.4	31.2
ϕ	0.43	Stable	Stable	Stable	Stable	Cannot Achieve Condition	Cannot Achieve Condition	Cannot Achieve Condition
	0.49	Stable	Stable	Stable	Stable	Stable	Stable	Stable
	0.54	Stable	Stable	Stable	Stable	Stable	Stable	Stable
	0.60	Stable	Stable	Stable	Stable	Stable	Stable	Stable
	0.65	Stable	Stable	Stable	Stable	Stable	Unstable	Unstable
	0.70	Stable	Stable	Stable	Stable	Unstable	Unstable	Stable
	0.76	Stable	Stable	Stable	Unstable	Unstable	Stable	Stable

Measurements include:

- Flow rates
- Dynamic pressure
- Surface temperatures
- Global heat release
- High-speed flame imaging

Stable
 Unstable
 Poor Stabilization
 Cannot Achieve Condition

Goals of Q1/Q2 testing:

- Quantify steady-state flame behavior and stability
- Develop methodologies for ensuring repeatability

$U = 22.5 \text{ m/s}$, $T_{\text{in}} = 200^\circ\text{C}$, fully premixed, unforced

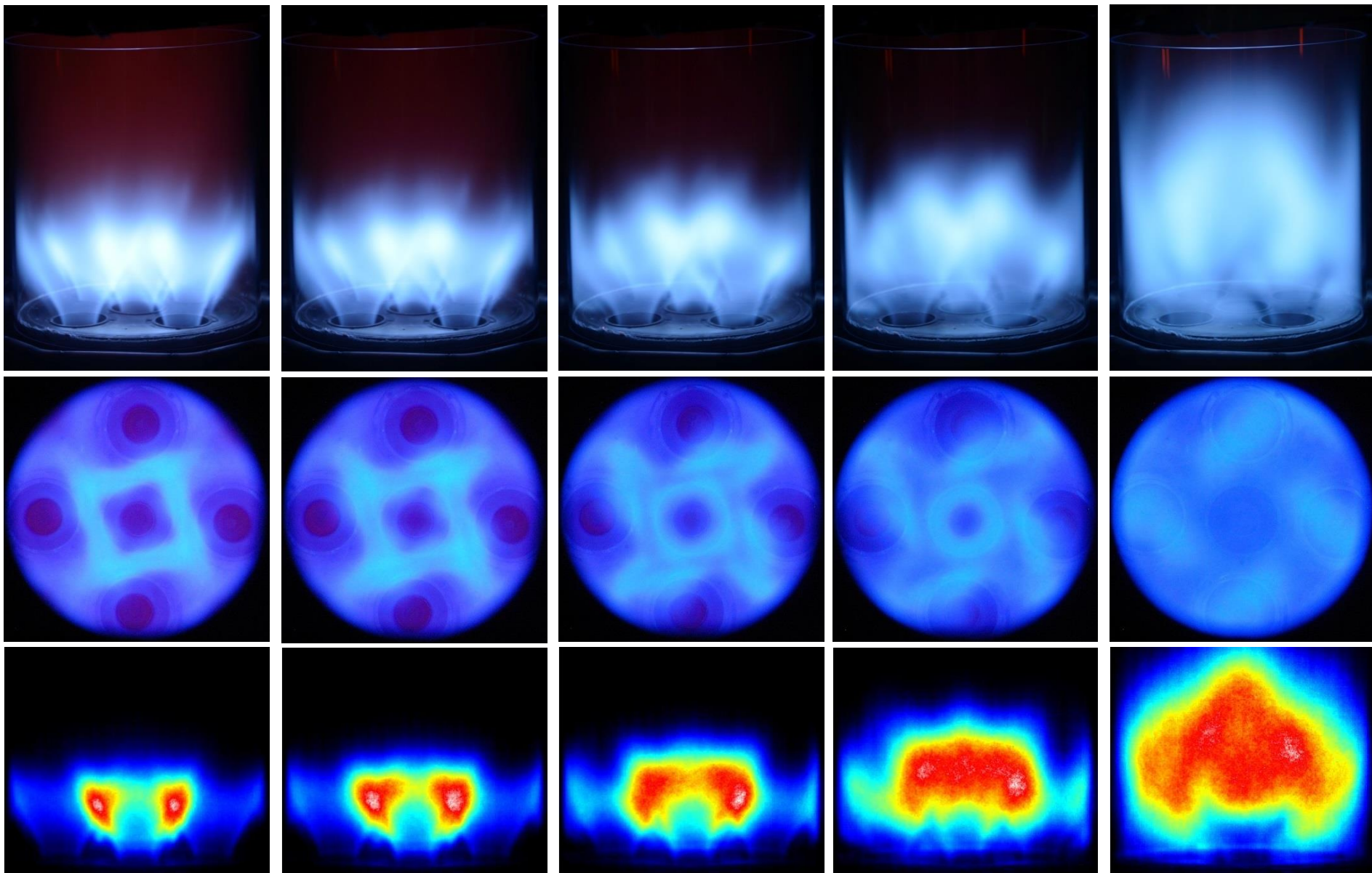
$\varphi = 0.65$

$\varphi = 0.60$

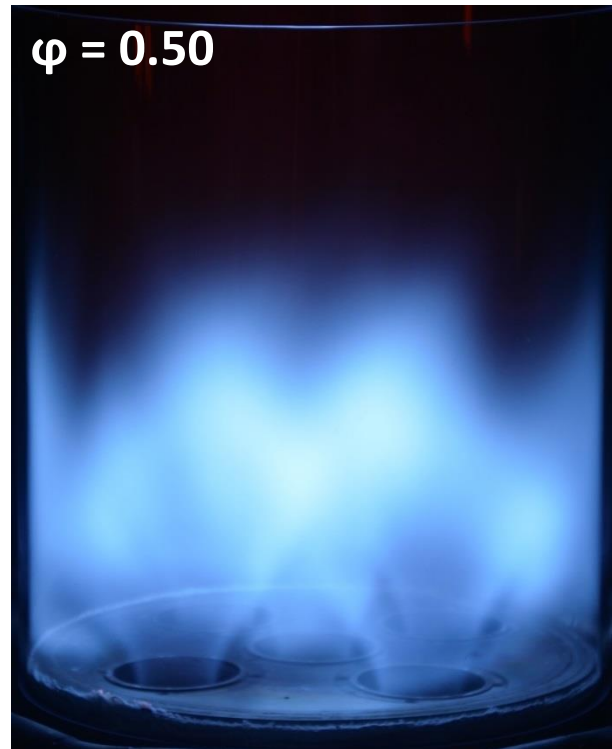
$\varphi = 0.55$

$\varphi = 0.50$

$\varphi = 0.45$



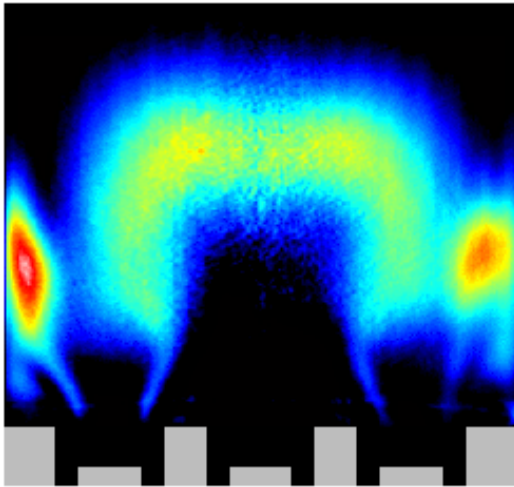
Instabilities may arise as a result of changes in flame shape and flame anchoring that occur with variation in equivalence ratio



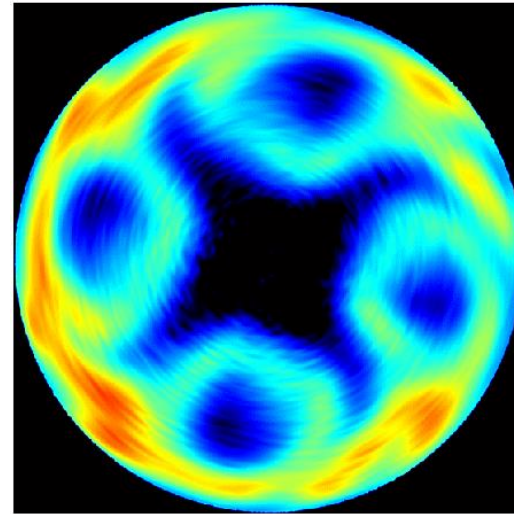
Photographs of multi-nozzle flame at $U = 25 \text{ m/s}$, $T_{\text{in}} = 200^\circ\text{C}$

To further investigate the structure of the multi-nozzle flame, 3-D image sets were obtained at $\phi = 0.60$ and $\phi = 0.48$

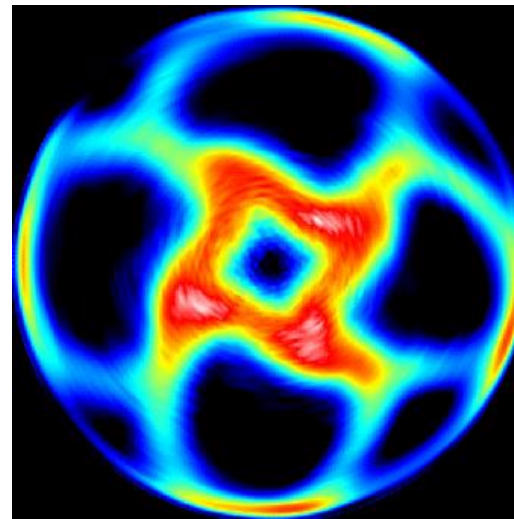
$\phi = 0.48$



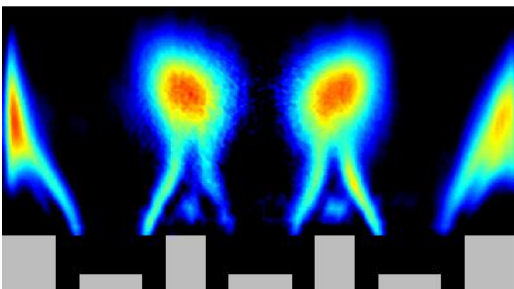
$\phi = 0.48$



$\phi = 0.60$



$\phi = 0.60$



Data from unforced and forced flames are available in a range of operating conditions

Stable	Unstable	Poor Stabilization	Cannot Achieve Condition
--------	----------	--------------------	--------------------------

Inlet temperature = 100°C								
		U (m/s)						
		15	17.5	20	22.5	25	27.5	30
ϕ	0.40							
	0.45							
	0.50							
	0.55							
	0.60							
	0.65							
	0.70							
	0.75							

Inlet temperature = 150°C								
		U (m/s)						
		15	17.5	20	22.5	25	27.5	30
ϕ	0.40							
	0.45							
	0.50							
	0.55							
	0.60							
	0.65							
	0.70							
	0.75							

Inlet temperature = 200°C								
		U (m/s)						
		15	17.5	20	22.5	25	27.5	30
ϕ	0.40							
	0.45							
	0.50							
	0.55							
	0.60							
	0.65							
	0.70							
	0.75							

Inlet temperature = 250°C								
		U (m/s)						
		15	17.5	20	22.5	25	27.5	30
ϕ	0.40							
	0.45							
	0.50							
	0.55							
	0.60							
	0.65							
	0.70							
	0.75							

An inlet temperature of 200°C and an inlet velocity of 25 m/s was chosen for the steady-state tests

Inlet temperature = 200°C								
		U (m/s)						
		15	17.5	20	22.5	25	27.5	30
ϕ	0.40							
	0.45							
	0.50							
	0.55							
	0.60							
	0.65							
	0.70							

Based on the stability maps of fully premixed operation, this condition was chosen as it enables both transition in flame structure and transition to instability by varying fuel flow rate

	Stable	Unstable	Poor Stabilization	Cannot Achieve Condition
--	--------	----------	--------------------	--------------------------

Stability map for GE-15 single-nozzle experiment (TPM)

	$T_{in} = 100^{\circ}\text{C}$			$T_{in} = 200^{\circ}\text{C}$			$T_{in} = 275^{\circ}\text{C}$	
ϕ	25 m/s	30 m/s	35 m/s	25 m/s	30 m/s	35 m/s	30 m/s	35 m/s
0.50				LBO	LBO	LBO	LBO	LBO
0.525		LBO	LBO	57 Hz	72 Hz	81 Hz	97 Hz	106 Hz
0.55	LBO	68 Hz	84 Hz	78 Hz	86 Hz	111 Hz	105 Hz	116 Hz
0.60	71 Hz	96 Hz	117 Hz	94 Hz	110 Hz	124 Hz	111 Hz	125 Hz
0.65	89 Hz	114 Hz	124 Hz	101 Hz	115 Hz	125 Hz	117 Hz	127 Hz
0.70	104 Hz	117 Hz	129 Hz	112 Hz	118 Hz	128 Hz	129 Hz	145 Hz

	stable		unstable		estimate lean blow-off
--	--------	--	----------	--	------------------------

Stability map for GE-15 single-nozzle experiment (FPM)

	Tin=100 C			Tin=150 C			Tin=200 C		
ϕ	20 m/s	25 m/s	30 m/s	20 m/s	25 m/s	30 m/s	20 m/s	25 m/s	30 m/s
0.50		LBO	LBO	LBO	LBO	LBO	LBO		LBO
0.55	LBO								
0.60									
0.65									
0.70									
0.75									

	stable	unstable	estimate lean blow-off
--	--------	----------	------------------------

Fuel injection strategy for staging

Two options for adding additional fuel to middle nozzle:

- (1) Inject fuel at swirler → technically premixed
- (2) Inject fuel at air manifold with a choke → fully premixed

Poravee showed using acetone PLIF, that the fuel and air are well mixed at the nozzle exit of the GE-15 nozzle

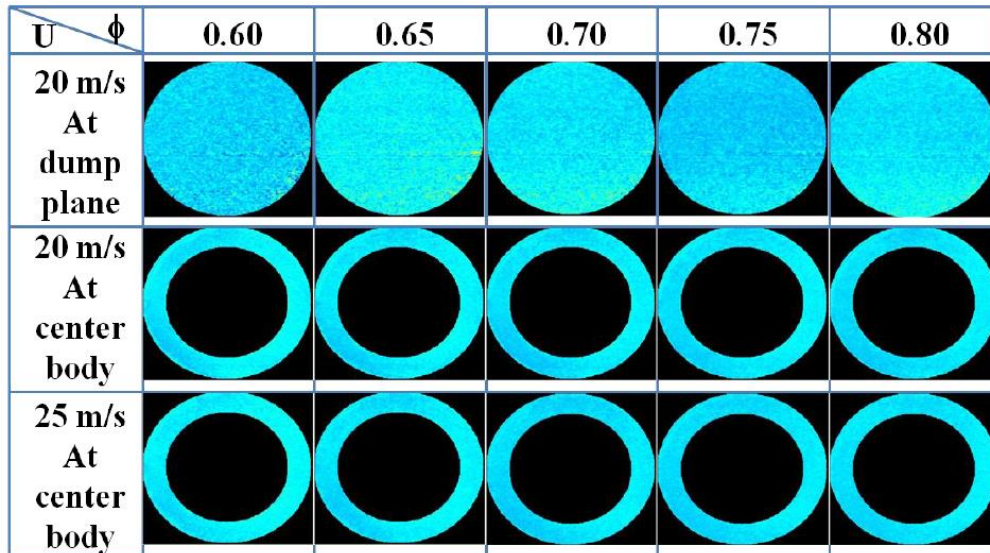
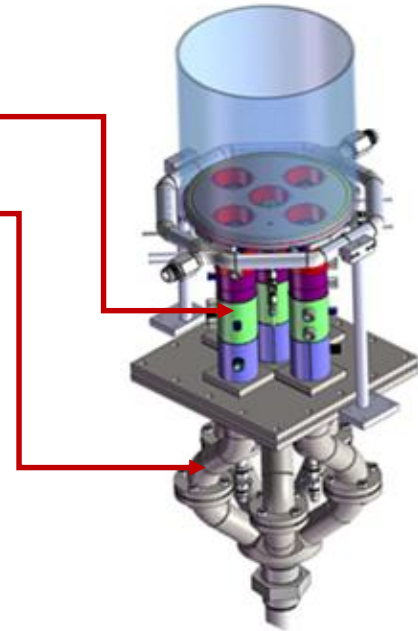


Figure B-4. Spatial distribution of fuel-air mixture results.

The main difference between these then becomes the type of governing mechanisms during the unstable flame case

Fuel injection strategy for staging

